

**IRFAN HUSSAIN**

**2009-NUST-MS-PHD-MTS-02**

**MS-62**

**DESIGN OF ELBOW JOINT FOR ABOVE ELBOW  
PROSTHESIS**



*Defining futures*

**COLLEGE OF  
ELECTRICAL AND MECHANICAL ENGINEERING  
NATIONAL UNIVERSITY OF SCIENCES AND TECHNOLOGY  
RAWALPINDI  
2011**

# College of Electrical & Mechanical Engineering



## THESIS REPORT

### DESIGN OF ELBOW JOINT FOR ABOVE ELBOW PROSTHESIS

Submitted to the Department of Mechatronics Engineering  
in partial fulfillment of the requirements  
for the degree of  
**Master of Engineering**  
in  
**Mechatronics**  
2011

#### Supervisor:

Dr. Adnan Masood

#### Submitted By:

Irfan Hussain

2009-NUST-MS-PHD-MTS-02

# TABLE OF CONTENTS

---

Acknowledgement.....	I
Abstract.....	II
List of Symbols.....	III
Table of Contents.....	IV
List of Figures.....	VIII
List of Tables.....	XI

## Chapter 1

## Introduction

---

1.1 Artificial Limb.....	2
1.2 Prosthesis .....	2
1.2.1 Types of Upper limb prosthesis .....	2
1.2.1.1 Transhumeral Prosthesis (Above Elbow) .....	2
1.2.1.2 Transradial Prosthesis (Below Elbow).....	2
1.2.1.3 Body Powered Elbow Prosthesis .....	3
1.2.1.4 Externally Powered Elbow Prosthesis .....	3
1.2.1.5 Myoelectric Prosthetic Limb .....	3
1.2.1.6 Switch-Controlled Prosthetic Limb .....	3

## Chapter 2

## Literature Review

---

2.1 Status of Elbow Prosthesis.....	5
2.1.1 Otto Bock Prosthesis .....	5
2.1.2 Utah Arm.....	8
2.1.2.1 Characteristics of Utah Arm.....	9



5.5 Planetary Gear Set.....	52
5.6 Planetary Gear Set applications and advantages.....	52
5.7 Working Principle .....	52
5.8 Driving Configuration of Planetary Gear Set.....	53
5.9 Harmonic Drives.....	54
5.10 Brief History of the Harmonic Drive Gearing.....	54
5.11 Components of harmonic drive.....	55
5.11.1 FLEXSPLINE .....	55
5.11.2 WAVE GENERATOR .....	55
5.11.3 CIRCULAR SPLINE .....	55
5.12 Principle of Operation.....	56
5.13 Driving Configurations .....	57
5.14 Advantages.....	59
5.14.1 Zero Backlash.....	59
5.14.2 Consistent Performance.....	59
5.14.3 High Positional Accuracy.....	59
5.14.4 High Torque-to-Weight Ratio.....	60
5.14.5 Affordable Precision.....	60
5.15 Harmonic Drive Applications .....	60
5.15.1 SCARA Robots.....	60
5.15.2 Light Weight Robots.....	61
5.15.3 Walking Robots.....	62
5.16 CSD Harmonic Drive Rating Table .....	63
5.17 Technical Terms .....	64
5.17.1 Definition of Rating.....	64
5.17.1.1 Rated Torque ( $T_r$ ).....	64
5.17.1.2 Limit for Repeated Peak Torque.....	64
5.17.1.3 Limit for Average Torque.....	64
5.17.1.4 Limit for Momentary Peak Torque.....	64
5.17.1.5 Maximum Input Speed, Limit for average input speed.....	65
5.17.1.6 Moment of Inertia.....	65
5.17.1.7 Strength and Life.....	65

5.17.1.8 Ratcheting phenomenon.....	66
5.17.1.9 CSD Ratcheting Torque (Nm) .....	66
5.17.1.10 Buckling Torque (Nm).....	67
5.17.1.11 The Life of a Wave Generator.....	67
5.17.1.12 Relative Torque Rating.....	68
5.18 Selection Procedure.....	69
5.18.1 Size Selection.....	69
5.18.2 Parameters.....	69
5.18.3 Normal Operating Pattern.....	70
5.18.4 Maximum RPM .....	70
5.18.5 Impact Torque.....	70
5.19 Flow Chart for selecting a size.....	71
5.20 Selection of my Harmonic Drive.....	72
5.20.1 Values of an each load torque pattern.....	72
5.21 Pro/Engineer (Wildfire 5.0) Model.....	74
5.22 How to Order.....	76

## **Chapter 6**

## **Conclusion and Recommendations**

---

Conclusion and Recommendations.....	77
-------------------------------------	----

## **Appendices**

---

Appendix A: Anthropometric data and Regression Equations.....	79
Appendix B: Selected Motor.....	82
Appendix C: Rechargeable Battery Pack.....	85
Appendix D: Smart Chargers For NiMH/NiCd Battery Packs.....	87

**CHAPTER 1**

**INTRODUCTION**

## **1. Introduction**

### **1.1 Artificial Limb**

Prosthesis is a device that is designed to replace, as much as possible, the function or appearance of a missing limb or body part. An artificial limb is a type of prosthesis that replaces a missing extremity, such as arms and legs. The type of artificial limb used is determined largely by the extent of an amputation or loss and location of the missing extremity. Artificial limbs may be needed for a variety of reasons, including disease, accidents, and congenital defects. A congenital defect can create the need for an artificial limb when a person is born with a missing or damaged limb. Industrial, vehicular, and war related accidents are the leading cause of amputations in developing areas, such as large portions of Africa. In more developed areas, such as North America and Europe, disease is the leading cause of amputations. Cancer, infection and circulatory disease are the leading diseases that may lead to amputation.

### **1.2 Prosthesis**

An artificial substitute for a missing body part such as an arm or leg, eye or tooth. Used for functional or cosmetic reasons or both.

- Upper limb prosthesis
- Lower limb prosthesis

#### **1.2.1 Types of Upper limb prosthesis**

There are different types of upper limb prosthesis.

##### **1.2.1.1 Transhumeral Prosthesis (Above Elbow)**

Above-elbow prosthesis consists of a single plastic upper arm shell, an elbow joint usually with incorporated locking mechanism, a plastic forearm and a wrist joint to which is attached a terminal device, either a hook or a hand.

##### **1.2.1.2 Transradial Prosthesis (Below Elbow)**

Below elbow prosthesis consists of forearm, wrist joint and terminal device.



### **1.2.1.3 Body Powered Elbow Prosthesis**

Body-powered prostheses (cables) usually are of moderate cost and weight. They are the most durable prostheses. However, a body-powered prosthesis is more often less cosmetically pleasing than a myo-electrically controlled type is, and it requires more gross limb movement

### **1.2.1.4 Externally Powered Elbow Prosthesis**

Prostheses powered by electric motors may provide more proximal function and greater grip strength, along with improved cosmesis. Patient-controlled batteries and motors are used to operate these prostheses. Externally powered prostheses require a control system. The two types of commonly available control systems are

### **1.2.1.5 Myoelectric Prosthetic Limb**

Myoelectric controlled prosthesis uses muscle contractions as a signal to activate the prosthesis. It functions by detecting electrical activity from select residual limb muscles, with surface electrodes used to control electric motors. Different types of myoelectric control systems exist.

### **1.2.1.6 Switch-Controlled Prosthetic Limb**

Switch Controlled externally powered prostheses utilize small switches, rather than muscle signals, to operate the electric motors. Typically, these switches are enclosed inside the socket or incorporated into the suspension harness of the prosthesis. A switch can be activated by the movement of a remnant digit or part of a bony prominence against the switch or by a pull on a suspension harness (similar to a movement a patient might make when operating a body-powered prosthesis). This can be a good option to provide control for external power when myoelectric control sites are not available or when the patient cannot master myoelectric control.

**CHAPTER 2**  
**LITERATURE REVIEW**

## **2 Literature Review**

For adults four different elbow units are available: the NY Electric Elbow, the Boston Elbow, the Utah Arm, and the Otto Bock Dynamic Arm. All four elbows differ in mechanical configuration, but all incorporate a turntable to allow for passive humeral rotation. These elbows have a limited active lifting capability. Heavier loads can be lifted in a passive manner by locking the elbow in place. However, the overload protection unit built into these elbow sets an upper limit to the load carrying capability

### **2.1 Status of Elbow Prosthesis**

Worldwide, every year the number of amputees increases in 150,000 to 200,000. Myoelectric prostheses are powered by the muscles electric signal taken from the residual limb. The ideal solution for the amputation would be the biological regeneration of the limb lost. So far, the technological advances do not allow this biological solution, so it is necessary to develop artificial systems to collaborate in the rehabilitation of the amputee in order to improve his or her quality life.

The need that upper limb prosthesis must cover depends on the type of amputation that the patient had suffered. The degree of the amputation goes from the fingers, the hand, and the wrist disarticulation, under the elbow with long, medium and short stump, elbow disarticulation, above the elbow with long, medium and short stump, shoulder disarticulation and scapular-thoracic disarticulation. Each one of them has different remnant movements and atomic structures that allow different possibilities for prosthesis design.

The brief history of myoelectric prosthesis and their main characteristics are

#### **2.1.1 Otto Bock Prosthesis**

Until the 1970's the socket design and attachment essentially consisted of gluing together and laminating the wooden parts of the prosthesis. Since then, a steady movement toward a more modular-type prosthesis has taken place. For many years the Otto Bock company based in Germany held the exclusive patent to the pyramid and ball attachment system that was the

foundation of endoskeleton modular system prosthesis. Over the years, other manufacturers have adopted their components, thus offering the prosthetist the ability to hybridize the Bock endoskeletal modular system to include several manufacturer components.

These interlinking components make possible the multifunctional prostheses we see in use today by amputees around the world. Without these innovative components, such hybridized prostheses would not be possible. Also the German Company Otto Bock manufactures myoelectric prostheses of hands. The Otto Bock hand weights 540 g and can perform a force of 140 N. These kinds of devices developed by Otto Bock are useful for the myoelectric prosthesis available in the market. Actually, the myoelectric hand of Otto Bock is a terminal device which is preferable for elbow prosthesis designers. For instance, Utah arm and Boston elbow are compatible with this terminal device. Three kinds of mechanical elbow products are currently offered to the patients.

The first is the elbow with toothed rack (figure 2.1), which is released thanks to a pushbutton actuated by the valid hand or by a cable.

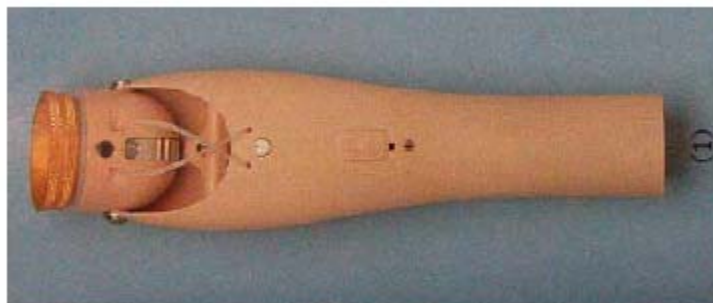


*Figure 2.1 Otto Bock Elbow with toothed profile*

The front sizes of this product are proposed by this company. There are many drawbacks: noise of the toothed rack, the limited number of positions of the front arm and the bad aesthetic of the pushbutton. The second elbow is the elbow with friction, which moves thanks to the friction of a spiral spring on the axis of the elbow. A cable ordered by the other shoulder actuates blocking: traction locks it, another unbolts it. It is more functional than the precedent, but maintains the position less firmly. In addition, it needs a double order from the amputee, which is not always easy to carry out. Third is an automatic elbow from OTTO BOCK. The front arm is

manufactured out of plastic and is not very solid. Its distal part (near to the wrist) is cylindrical and is simply cut to the length of the healthy member.

The Otto Bock Dynamic Arm shown in Figure 2.2 features an electronically controlled variable gear mechanism that allows for continuous adjustment of the transmission ratio between the motor and the arm. The transmission ratio depends on the external load, the flexion angle of the elbow, and the relevant muscular signals of the user. The variable gear mechanism, in conjunction with an integrated forearm balance system, makes the arm about twice as fast as other electric elbows. The Dynamic Arm also features a free swing mode and automatically locks in every desired elbow flexion angle. The Dynamic Arm is a microprocessor controlled elbow joint driven by an electric motor that can be controlled by the user with great precision. The speed of flexion and extension of the elbow are proportionately controlled. Likewise, pronation and supination of the wrist can be controlled proportionately via the integrated electronics of the Electric Wrist Rotator.



*Figure 2.2: The Otto Bock Dynamic Arm, an electric elbow prosthesis and terminal device*



*Figure 2.3: The Otto Bock Dynamic Arm, the electric elbow part*

### **2.1.2 Utah Arm**

The Utah artificial arm was developed at the university of Utah in a laboratory started in 1947 by Dr. Stephen C. Jacobsen, Ph.D , and now called center for Engineering Design. The first version of the self-contained myoelectric elbow unit was introduced in December 1980.

Since 1985, amputees have been fitted with the proportional 12 V Utah hand controller, which is used with the Otto Bock hand mechanism. The 6V version replaced it in 1989. In contrast to the commonly used “myo switch’ type of control, which simply turns the hand “ON” in one direction or the other, the proportional control provides the user with more sensitive slow and fast control of the hand, depending on the strength of muscle contraction. Below elbow

fittings of the system have installed the battery packs placed on the side of the forearm. By then the system was appropriate for middle forearm or shorter amputations or for candidates of juvenile age or older. Powered wrist rotation was also available using the Otto Bock electric wrist. Control might be transferred between the wrist and hand using an external switch. The next version transferred control between hand and wrist by a rapid muscle contraction.

Since 1981, the Utah Arm has been the premier myoelectric arm for above elbow amputees. In 1987, Motion Control released the Utah Arm 2, and in 2004, Motion Control introduced microprocessor technology into the Utah Arm 3 (U3), which delivers the same sensitivity, proportional control of elbow, hand and wrist letting the patient to move the arm and hand slowly or quickly in any position. This functionality provides more natural response with less effort for the patient than the traditional on/off movement. Since the Utah Arm 3 has two microprocessors, two functions can be controlled at once, producing a more natural movements are typically used, although supinator muscles have also been utilized in some very short below elbow amputees. When fitted to above elbow patients, biceps and triceps sites are typically used. Higher level amputees may require training and careful muscle selection.

About the socket there are different kinds of fitting; the total contact socket in which suspension is provided by harness, a silicon acromial cap with chest strap suspension which transfers more of the prosthesis load to the shoulder, a self suspending suction type, socket.

#### **2.1.2.1 Characteristics of Utah Arm**

The size and strength of the prosthesis represent important characteristics that will impact whether the patient uses the prosthesis or not. The forearm length can be shortened up to 20.32 cm. It supports a load during activity of 1kg in the terminal device, hand or hook. The arm weight 913 g without hand and the hand weights 450 g, plus glove; the individual should be capable of supporting this amount of weight. The load limit is 22.7 kg with the elbow in 90 deg flexion and 15.9 kg in the extended arm. The active lift is 1 kg in the terminal device and using a fully charged battery. The operation temperature is from 0 centigrade to 44 centigrade; the standard length of the forearm is 27.3 cm.

Currently Utah Arm elbow, without load can rotate from 0 deg to 135 deg in 1.2 Seconds, approximately. The last model of the Utah Arm, distributed by Motion Control Inc, emulates

simultaneous movements of the arm and the hand and connects to the body by using surface electrodes; plus a computational interface to carry out the arm calibration.

The mechanical drive train of the Utah Arm is located within the injection molded plastic forearm enclosure. The elbow can be locked in 22 positions throughout the range of motion. Elbow locking is engaged whenever the elbow is held stationary for a set period of time. Unlocking occurs either with so-called rate-control, i.e. a rapid co-contraction of the controlling muscles, or with threshold-control, i.e. a slower contraction of at least one control muscle. In addition unlocking is possible by the actuation of a momentary switch that can also be used for locking. Lock control by the switch is always available; rate control or threshold control is mutually exclusive and are determined by an adjustment in the electronics. A powered free swing mode, in which the motor actively flexes and extends the elbow to compensate for the electromechanical inertia of the drive mechanism, is available when the elbow is unlocked and no myo-electric signals are present. The battery and the electronics are located in the upper arm part of the system.

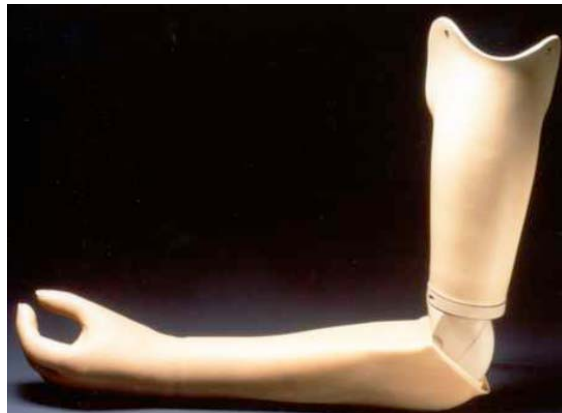


*Fig 2.4: The Utah Arm, electric elbow prosthesis for adults.*

### **2.1.3 The NY Electric Elbow**

The NY Electric Elbow shown in Figure designed at the NY-University is marketed by the Hosmer Dorrance Corporation and is available in two sizes, both for exoskeleton or endoskeleton applications. All versions use the same motor and drive configuration, located in the upper arm part of the system. A pawl-type locking mechanism is provided to automatically lock the elbow whenever the control signal ceases. The elbow also features full range-of-motion



free swing: the elbow drive disengages when the elbow is fully extended. The elbow automatically engages again when flexed. The battery pack and the electronics can be located at any location convenient.



*Figure 2.5: NY Electric Elbow, Exoskeletal*



*Figure 2.6: NY Electric Elbow, Endoskeletal*

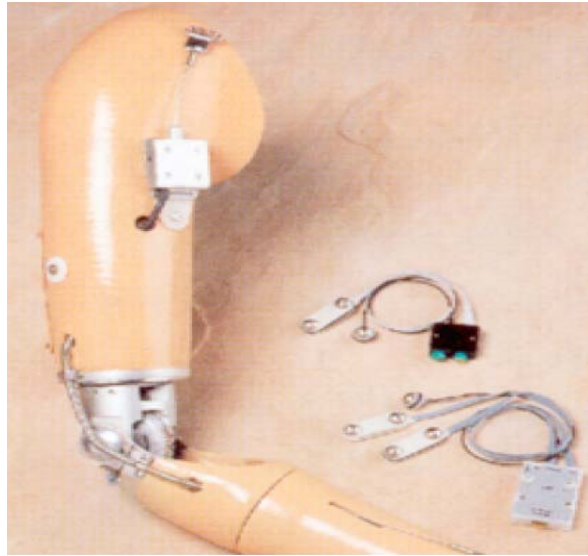


*Figure 2.7: The NY electric elbow for adults*

#### **2.1.4 Boston Elbow**

Since Liberty Mutual was founded as a casualty insurance company in 1912, the prevention of accidents and the resulting financial loss to policyholders has been a primary corporate goal. Since 1961 the Research Center has been developing myoelectrically controlled prosthetic arms to replace lost limbs. In 1969, Liberty Mutual began supplying industrial accident victims with the Boston Elbow. In 1979, when the Boston Elbow had been proven a reliable prosthetic component, the Research Center began offering it to prosthetists throughout the United States. Several hundred Boston Elbows are now in use.

To control the elbow joint, the Boston Elbow uses two muscles, usually the biceps and the triceps. With this strategy, an amputee flexes his remaining muscles as if to move the missing arm. Sensitive electrodes on the skin surface detect electric activity in the underlying muscles, and these signals control the speed and direction of the electric motor that moves the prosthetic limb.

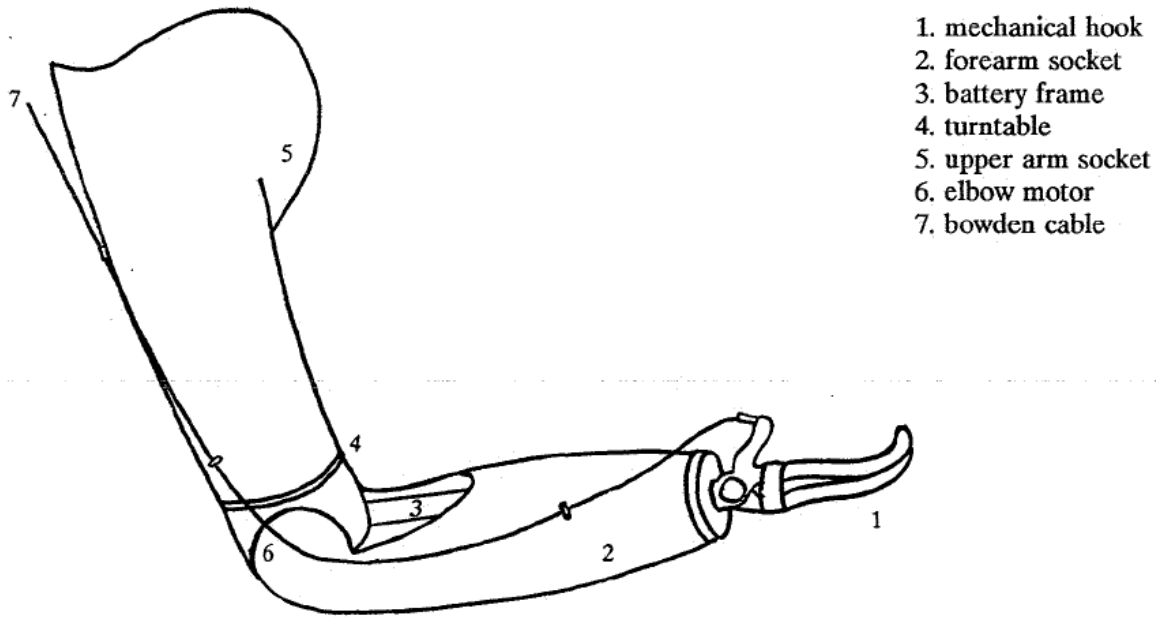


*Figure 2.8: The Boston Elbow*

The Boston Elbow is a system that offers the prosthetics and amputee many choices for fitting and control. The control modes vary from simple switch control to myoelectric control of three functions by just two muscles. All choices, however, use the same elbow mechanism, rechargeable batteries, high-speed battery charger, and power-control circuitry. The most important element in the Boston Elbow is a sealed drive contained in a rugged housing. A DC motor located in this elbow drive runs the Boston Elbow.

The speed of the motor is proportional to muscle activity. An advantage of the Boston Elbow over most other elbows is that it locks and unlocks automatically. The elbow is locked except when the motor is activated by the amputee. Attached to the drive is a forearm-frame, which holds the battery and control unit. The forearm itself slides over this assembly. The size of the forearm duplicates the user's sound side dimensions. The Boston Elbow offers different options for the hand. Besides the mechanical hook electrical hands and grippers are used. Every option has its own advantages and disadvantages (i.e. weight, required body-motion for control, control modes and cosmetic aspects).

The Boston digital arm system was introduced in 2001. The system incorporates microprocessor technology for improved performance and patient adjustment. It can control up

to four other prosthetic devices in addition to the elbow itself, like hand, wrist rotators, shoulder lock actuator, etc. The terminal device is compatible with Otto Bock electric hand, centri electric hand Steeper electric hand, Otto Bock Greifer, Steeper powered gripper, body powered split-hooks, and Otto Bock electric wrist rotator.

The Boston digital arm system evaluates the patient for suitable muscle sites and then tries various control strategies until a proper one is found. This is accomplished through user-friendly graphical interface screen software. The software actualizes the control strategy by downloading it to the prosthesis in less than 10 seconds. This software is also useful to easily diagnose problems and often fix it.

#### **2.1.4.1 Characteristics of Boston elbow**

The Boston elbow is a myoelectric prosthesis of elbow with one single degree of freedom; the elbow flexion. It reproduces the active movement of the human elbow flexion and extension, but not of course, other forearm movements such as pronation, supination and flexion or extension at the wrist. Also, it connects to the arm using superficial electrodes. The myoelectric hand and the wrist rotator of Otto Bock could be used as a terminal device. In addition, a divided hook terminal device activated by a cable could be used with this elbow. It is endoskeleton prosthesis.

The Boston Elbow looks like a complete arm, which extends from the wrist (to which various hooks and artificial hands may be attached) to a socket that fits the stump, but only the elbow joint moves. Although any muscle can provide an EMG signal, the Boston Elbow is designed to tap residual biceps and triceps muscles, precisely those that would ordinarily flex and extend the arm. Thus an amputee's control of the prosthesis imitates control of the natural elbow.

The Boston Elbow is both myoelectric and proportional. So it moves at speeds directly proportional. So it moves at speeds directly proportional to the intensity of muscle contraction by the amputee. The forearm houses the batteries and electronics and offers the wearer a choice of terminal devices: a mechanical hook or hand controlled with a roll of the amputee's shoulder, or an electric or myoelectric hook or hand with switch control. The prosthesis has been designed so that hook and hand are interchangeable and may be used by the same wearer at different times.

The current Boston Elbow weighs 1.13 kg. It will lift 2.27 kg and hold something over 22.65 kg in locked position. A fully charged battery will power the device for about 8 hours. The prosthesis has a range of 145 degrees. That is full flexion is 145 degrees from full extension, and this distance is traveled in a minimum of a second. The Boston Elbow has a 30-degree free swing that lends it a more natural appearance.



*Figure 2.9 The Boston Digital Arm, electric elbow prosthesis for adults.*

## 2.2 Characteristics of Some Adult Electric-Powered Elbows

Characteristic	Boston Elbow	NY Electric Elbow	Utah Arm ( Elbow )
Turntable Diameter	7.3cm( 2.9 in)	7.1 cm ( 2.8 in)	7.0 cm(2.8 in)
Weight	0.96 kg	0.55 to 0.62 kg	0.91kg
Maximum lift capacity	5.9 Nm	3.4 Nm	4.3 Nm
Passive (Locked) lift capacity	68Nm	24.4 to 27.1 Nm	68 Nm
Range of motion	135 degrees	135 degrees	135 degrees
Speed ....no load	123 degrees/sec (20.5 rpm)	100 degrees/sec	112.5 degrees/sec
Speed---with counter Torque	60.7 degrees/sec.with counter torque of 1.4 Nm	56.5 degrees/sec..with counter torque of 1.7 Nm	
<b>Costs</b>			
Elbow	\$3,500		\$10,000
Fitting and Other Costs	\$6,000		\$10,000
Total	\$9,500		\$20,000

Annual repair	\$250		\$150
Service Life	5 years		6 years

*Table 2.1: Characteristics of Some Adult Electric-Powered Elbows*

## **CHAPTER 3**

### **MODEL OF HUMAN ARM**

#### **Approach 1: By Using Body Linage System**



### **3 Model of Human Arm**

#### **3.1 Motivation**

Athletic performance, work environment interaction, and medical sciences involving rehabilitation, orthotics, prosthetics, and surgery rely heavily on the analysis of human performance. Analyzing human motion allows for a better understanding of the anatomical and physiological processes involved in performing a specific task, and is an essential tool for accurately modeling intrinsic and extrinsic biodynamic behaviors. Analytical dynamic models (equations of motion) of human movement will assist the researcher in identifying key forces, movements, and movement patterns to measure, providing a base or fundamental model from which an experimental approach can be determined and the efficacy of initially obtained data can be evaluated. At times, the fundamental model may be all that is required if laboratory or field-based measurements prove to be costly and impractical. Finally, it permits the engineer to alter various assumptions and/or constraints of the problem and compare the respective solutions, ultimately gaining an overall appreciation for the nature of the dynamics.

#### **3.2 Mechanical Model of the Human Arm**

A Mechanical Model that describes the torque and forces on the shoulder joint for different position and movements of the arm in the sagittal plane. The calculation of the torques and forces on the shoulder joint for different position and movements of the arm is very important, especially for high level above elbow amputees, who have little support area between their stump and the artificial arm.

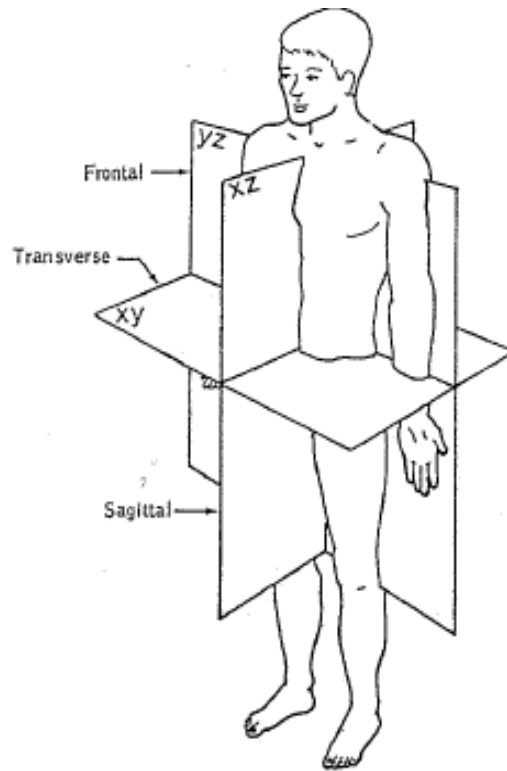


*Figure 3.1 Anatomical planes*

### **3.3 The Body Linkage System**

A description of the body as a linkage system (figure 3.2) provides a basic model to study the motion and posture of the body and its respective segments. Links are considered straight lines that connect the center of rotation on one side of human skeleton segments with the center of rotation on the other side or with the end. When dealing with limbs, the length of segments and links generally corresponds.

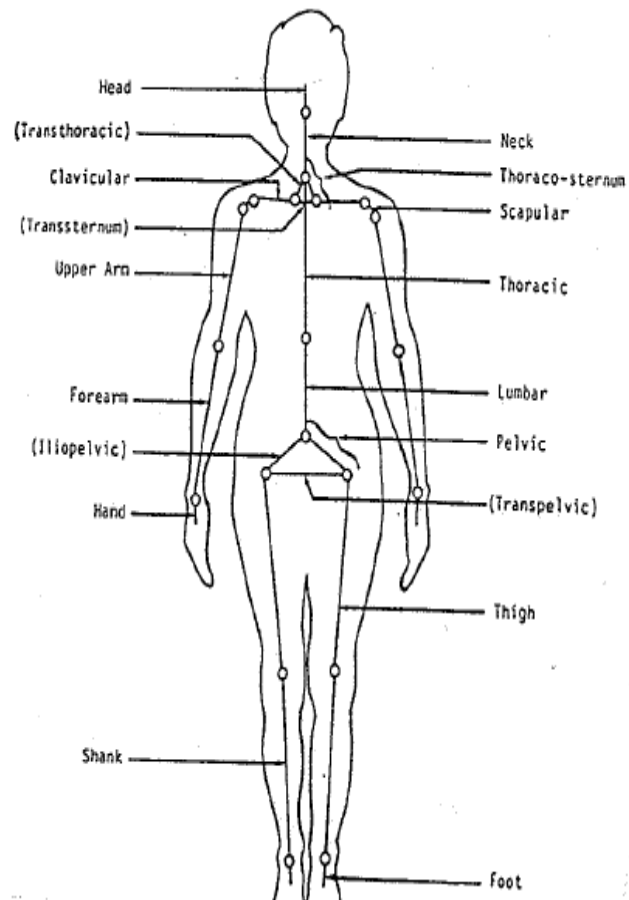


*Figure 3.2 The body linkage system*

The arm is divided in three links

- The upper arm (humerus) link is a straight line between the glenohumeral and elbow joint center of rotation.
- The forearm (radius and ulna) link is a straight line between the elbow and wrist
- The hand link is a straight line between the wrist joint center of rotation and the center of mass of the hand.

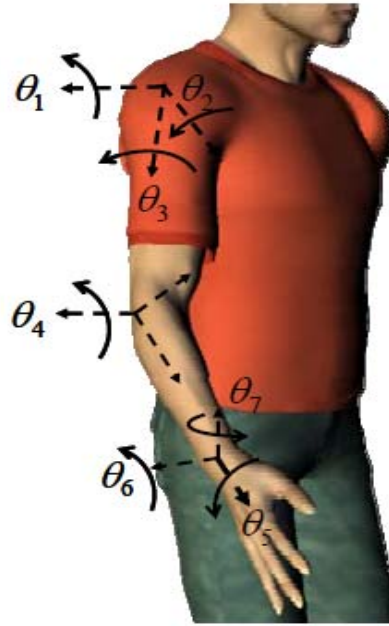


Figure 3.3 Shoulder, elbow and wrist joint

### 3.4 Weight distribution of the human arm

To determine the weight distribution of the human arm, data was selected from anthropometric data assembled by NASA. Values of link lengths, segments weight, mass centers and moments of inertia are calculated with the regression equations.

#### 3.4.1 Anthropometric data and Regression Equations

Anthropometric data and regression equations are given in appendix A.

The arm is represented by two vectors in series to derive a simple model of an arm (figure 3.4). The first vector  $\overline{OC}$  represents the upper arm and the second vector  $\overline{PC}$  represents the forearm including the hand. The points O and C represent the shoulder and elbow joint respectively. The model does only include movements in the sagittal plane and does not include wrist and hand movements. In addition the length of the vectors  $\overline{OC}$  and  $\overline{PC}$  are considered constant.

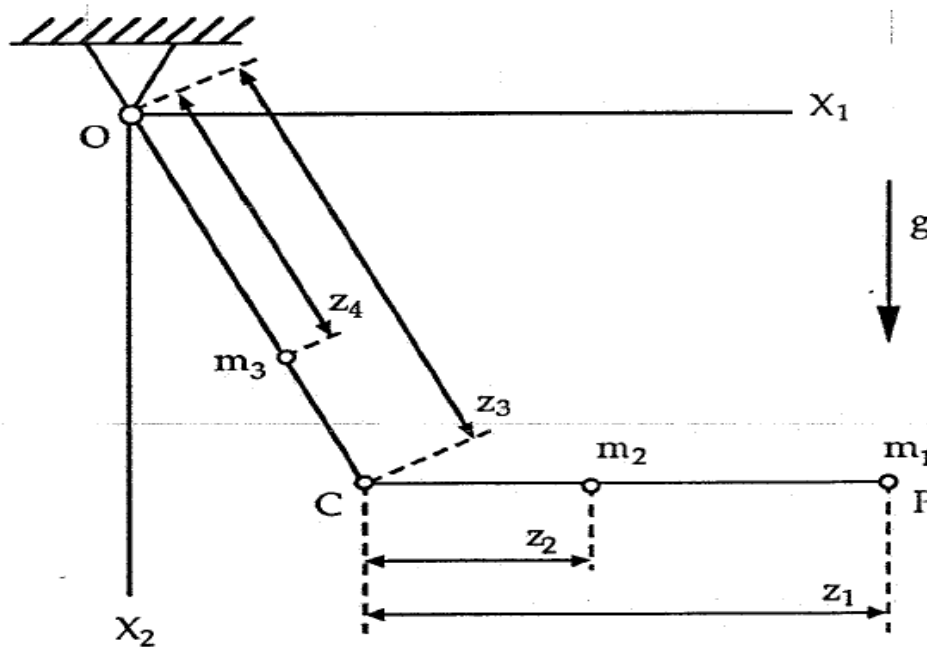


Figure 3.4 Positions of mass centers of arm segments

Vector  $\overline{OC}$  = Upper arm

Vector  $\overline{PC}$  =Forearm including hand

Point O=Shoulder Joint

Point C=Elbow Joint

$m_1$  = Hand

$m_2$  = Forearm

$m_3 = \text{Upper arm}$

$g = \text{gravity (m/s}^2\text{)}$

Assumptions:

- The segments are symmetric about the length axis.
- Measured from center of rotation of elbow motor.
- Because of the minimum weight, the cable-operated hook is most used by high-level amputees.
- Measured from the proximal end.

The equilibrium of forces and torques for only one mass  $m_i$  ( $i=1, 2$  and  $3$ ), with a moment of inertia  $J_i$  is given in figure 3.5.

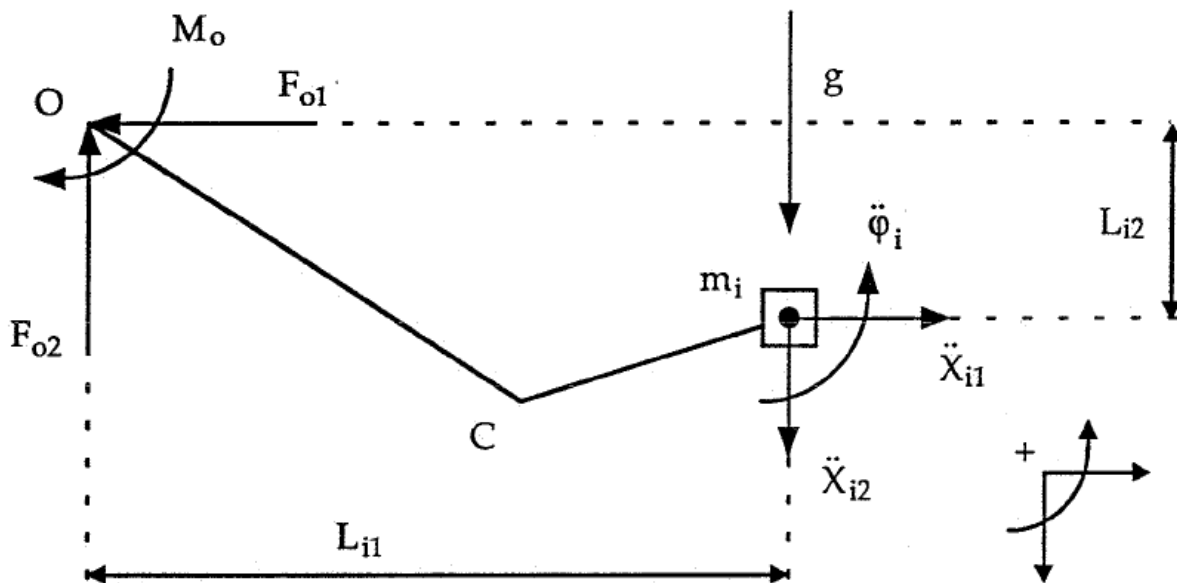


Figure 3.5 Equilibrium of one segment

$\ddot{X}_1, \ddot{X}_2$ , and  $\ddot{\phi}$  are accelerations caused by movements of the shoulder joint and elbow motor.  $F_{O1}, F_{O2}, M_O$  are the reaction forces and reaction torque on the shoulder joint respectively.

The equilibrium equations;

$$\Sigma F_1 = 0 \quad (3.1)$$

$$\Sigma F_2 = 0 \quad (3.2)$$

$$\Sigma M = 0 \quad (3.3)$$

$$\Sigma F_{o1} = m_i \ddot{x}_{i1} \quad (3.4)$$

$$\Sigma F_{o2} = m_i \ddot{x}_{i2} + m_i g \quad (3.5)$$

$$\Sigma M_o = m_i \ddot{x}_{i1} L_{i2} - m_i \ddot{x}_{i2} L_{i1} - m_i g L_{i1} + J_i \ddot{\theta}_i \quad (3.6)$$

In matrix-notation that is

$$F_0 = \begin{bmatrix} F_{o1} \\ F_{o2} \end{bmatrix} = m_i \begin{bmatrix} \ddot{x}_{i1} \\ \ddot{x}_{i2} \end{bmatrix} + m_i \begin{bmatrix} 0 \\ g \end{bmatrix} \quad (3.7)$$

$$M_0 = \begin{bmatrix} L_{i1} \\ L_{i2} \end{bmatrix}^T \begin{bmatrix} 0 & -1 \\ 1 & 0 \end{bmatrix} \begin{bmatrix} F_{o1} \\ F_{o2} \end{bmatrix} + J_i \ddot{\theta}_i \quad (3.8)$$

To study the kinematics of a system of two vectors that rotate with respect to each other, it is convenient to consider the motion of one vector  $\overline{PC}$  relatively to a moving frame of reference  $x_1 x_2$  attached to the other vector  $\overline{OC}$  that is rotating in a fixed frame of reference  $X_1 X_2$ . The respective  $x_1$  – axis and  $x_2$  – axis are perpendicular to vector  $\overline{OC}$ .

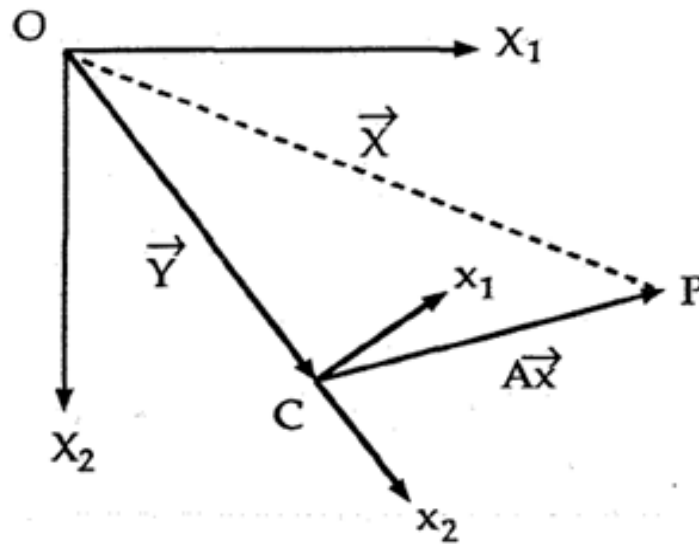


Figure 3.6 Vector Model of the Arm

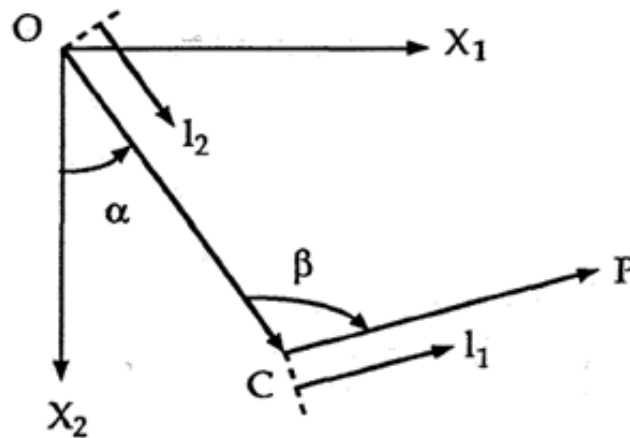


Figure 3.7 Definitions of positive angles and directions

- $\alpha(t) = \alpha$ ; is the angle between vector Y and the  $X_2$ -axis ( $-50 < \alpha < 180$ ).
- $\beta(t) = \beta$ ; is the angle between Y and AX ( $0 < \beta < 180$ ).
- $l_1$  is the distance from the elbow joint to any point on the forearm ( $0 < l_1 < z_1$ ).
- $l_2$  is the distance from the shoulder joint to any point on the upper arm ( $0 < l_2 < z_3$ ).
- Vector  $\overrightarrow{OP} = \vec{X}$ ; describes the position of point P in regard to O in the fixed frame.
- Vector  $\overrightarrow{CP} = \vec{x}$ ; describes the position of point P in regard to C in the moving frame.



The rotational relation between the two frames of reference is given by the matrix A. Let  $\alpha_{ij}$  be the angle between the  $X_i$ -axis and  $x_i$ -axis, then

$$A = \begin{bmatrix} \cos(\alpha_{11}) & \cos(\alpha_{12}) \\ \cos(\alpha_{21}) & \cos(\alpha_{22}) \end{bmatrix} \quad (3.9)$$

Vector  $\vec{OC} = \vec{Y}$ ; describes the translation of the moving frame with respect to the fixed frame of reference.

The relation  $\vec{OP} = \vec{CP} + \vec{OC}$  can now be written as

$$\vec{X} = \vec{AX} + \vec{Y} \quad (3.10)$$

By differentiating, we can get the equation for the velocity

$$\dot{\vec{X}} = \dot{A}\vec{x} + A\dot{\vec{x}} + \dot{\vec{Y}} \quad (3.11)$$

$$\ddot{\vec{X}} = \ddot{A}\vec{x} + 2\dot{A}\dot{\vec{x}} + A\ddot{\vec{x}} + \ddot{\vec{Y}} \quad (3.12)$$

$$A = \begin{bmatrix} \cos(\alpha) & \cos(\frac{\pi}{2} - \alpha) \\ \cos(\frac{\pi}{2} + \alpha) & \cos(\alpha) \end{bmatrix} \quad (3.13)$$

$$A = \begin{bmatrix} \cos(\alpha) & \sin(\alpha) \\ -\sin(\alpha) & \cos(\alpha) \end{bmatrix} \quad (3.14)$$

$$\vec{x} = \begin{bmatrix} l_1 \cos(\beta - \frac{\pi}{2}) \\ l_1 \sin(\beta - \frac{\pi}{2}) \end{bmatrix} \quad (3.15)$$

$$\vec{x} = \begin{bmatrix} l_1 \sin(\beta) \\ -l_1 \cos(\beta) \end{bmatrix} \quad (3.16)$$

$$\vec{Y} = \begin{bmatrix} l_2 \cos(\alpha) \\ l_2 \sin(\alpha) \end{bmatrix} \quad (3.17)$$

By differentiating

$$\dot{A} = \begin{bmatrix} -\sin(\alpha) & \cos(\alpha) \\ -\cos(\alpha) & -\sin(\alpha) \end{bmatrix} \quad (3.18)$$

$$\ddot{A} = \begin{bmatrix} -\cos(\alpha) & -\sin(\alpha) \\ \sin(\alpha) & -\cos(\alpha) \end{bmatrix} \quad (3.19)$$

$$\dot{\vec{x}} = \begin{bmatrix} l_1 \cos(\beta) \\ l_1 \sin(\beta) \end{bmatrix} \quad (3.20)$$

$$\dot{\vec{x}} = \begin{bmatrix} l_1 \cos(\beta) \\ l_1 \sin(\beta) \end{bmatrix} \quad (3.21)$$

$$\ddot{\vec{x}} = \begin{bmatrix} -l_1 \sin(\beta) \\ l_1 \cos(\beta) \end{bmatrix} \quad (3.22)$$

$$\dot{\vec{Y}} = \begin{bmatrix} -l_2 \sin(\alpha) \\ l_2 \cos(\alpha) \end{bmatrix} \quad (3.23)$$

$$\ddot{\vec{Y}} = \begin{bmatrix} -l_2 \cos(\alpha) \\ -l_2 \sin(\alpha) \end{bmatrix} \quad (3.24)$$

As

$$\dot{\vec{X}} = \dot{A}\vec{x} + A\dot{x} + \dot{Y} \quad (3.25)$$

$$\ddot{\vec{X}} = \ddot{A}\vec{x} + 2\dot{A}\dot{x} + A\ddot{x} + \ddot{Y} \quad (3.26)$$

$$\begin{aligned} \ddot{\vec{X}} = & \begin{bmatrix} -\cos(\alpha) & -\sin(\alpha) \\ \sin(\alpha) & -\cos(\alpha) \end{bmatrix} \begin{bmatrix} l_1 \sin(\beta) \\ -l_1 \cos(\beta) \end{bmatrix} + 2 \\ & \begin{bmatrix} -\sin(\alpha) & \cos(\alpha) \\ -\cos(\alpha) & -\sin(\alpha) \end{bmatrix} \begin{bmatrix} l_1 \cos(\beta) \\ l_1 \sin(\beta) \end{bmatrix} + \begin{bmatrix} \cos(\alpha) & \sin(\alpha) \\ -\sin(\alpha) & \cos(\alpha) \end{bmatrix} \begin{bmatrix} -l_1 \sin(\beta) \\ l_1 \cos(\beta) \end{bmatrix} + \\ & \begin{bmatrix} -l_2 \cos(\alpha) \\ -l_2 \sin(\alpha) \end{bmatrix} \end{aligned} \quad (3.27)$$

Where

$$-50 < \alpha < 180 \text{ degree}$$

$$0 < \beta < 180 \text{ degree}$$

$$0 < l_1 < z_1 \text{ (The distance from the elbow joint to any point on the forearm, } z_1 = 0.31 \text{ m)}$$

$$0 < l_2 < z_3 \text{ (The distance from the shoulder joint to any point on upper arm, } z_3 = 0.27 \text{ m)}$$

The only unknown variable in figure 3.5 is the angular acceleration  $\ddot{\phi}$ . From figure 3.5, it can be seen that

For the segments in the forearm

$$\ddot{\phi} = \ddot{\alpha} - \ddot{\beta} \quad (3.28)$$

And for the segments in upper arm

$$\ddot{\phi} = \ddot{\alpha} \quad (3.29)$$

Summation of the forces and torques of all the elements results in the total load on the shoulder joint.

$$F_{\text{tot}} = \sum_{i=1}^3 F_i \quad (3.30)$$

$$M_{\text{tot}} = \sum_{i=1}^3 M_i \quad (3.31)$$

### 3.5 Mechanical model of the Boston Elbow

The assumption that the upper arm socket fits perfectly over the stump and does not move with respect to the stump, allows to make a model for the Boston Elbow that is similar to the model of the human arm. The mass centers of the particular segments are given in figure 3.8.

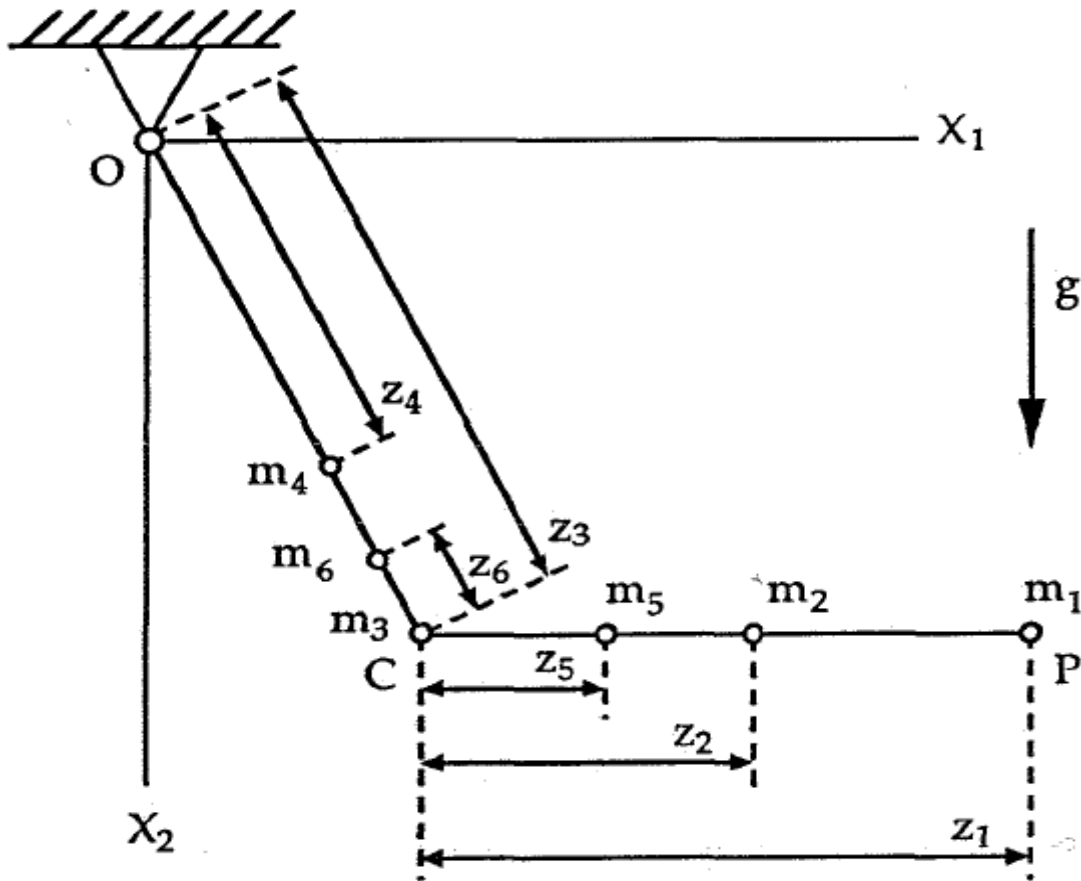


Figure 3.8 Positions of mass centers of Boston Elbow segments

$m_1$  = Hand

$m_2$  = Forearm cover

$m_3$  = elbow motor

$m_4$ =upper arm cover

$m_5$ = battery in forearm

$m_6$ =battery in upper arm

$g$  = gravity (m/s<sup>2</sup>)

The distance  $Z_5$  to the mass center of the forearm cover, battery frame and control board together, is determined with formula

$$x_{tot} = \frac{1}{\sum m_n} * \sum x_n * m_n \quad (3.32)$$

$x_{tot}$ = mass center of a system of n masses

$x_n$ = mass center of individual parts

When the battery is placed in the upper arm socket ( $m_6$ ),  $z_6$  represents the distance from the mass center of the battery to the elbow motor.

When the battery is placed in the fore arm socket ( $m_5$ ),  $z_5$  represents the distance from the mass center of the battery to the elbow motor.

In order to describe the Boston Elbow segments as rigid bodies, the moments of inertia need to be taken into account. The segments are approximated by the common geometric shapes given in below table.

$m_1$	Hand	solid circular cylinder
$m_2$	Forearm	pipe
$m_3$	Motor	Solid circular cylinder
$m_4$	Upper arm socket	pipe
$m_5$	Regular battery Pack	Solid rectangular prism

$m_6$	Circular battery pack	Thick-wall pipe
-------	-----------------------	-----------------

Table 3.1 Approximated common geometric shapes for segment

The radii correspond to average thickness of the Boston Elbow segments.

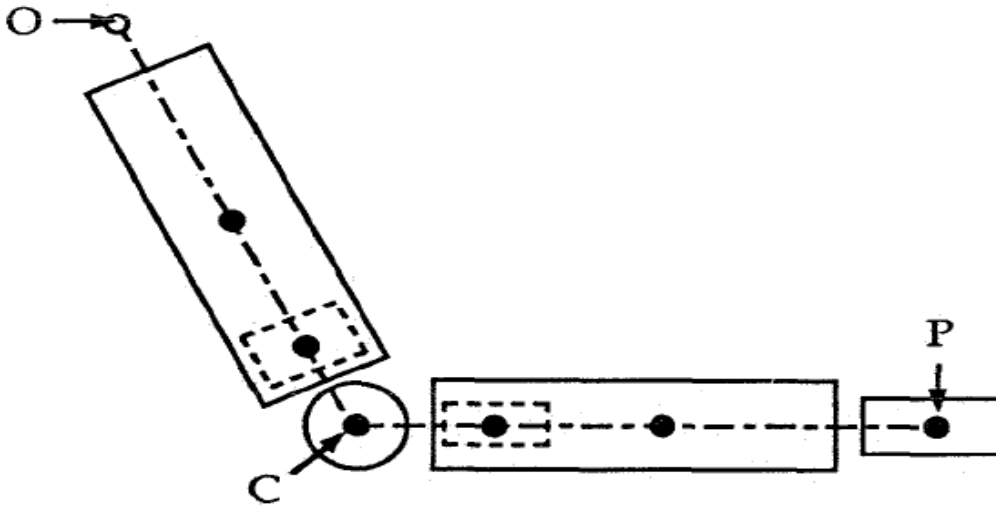
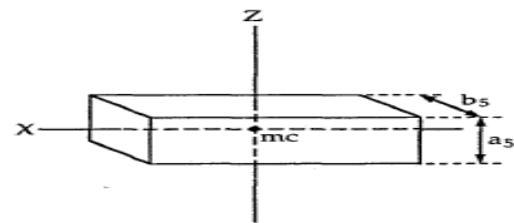


Figure 3.9 Approximated model of the Boston Elbow

A definition of moments of inertia ( $J_i$ ) around the mass center for every segment  $m_i$  ( $i = 1, 2, \dots, 6$ ), is found by using the moments of inertia for common geometric shapes

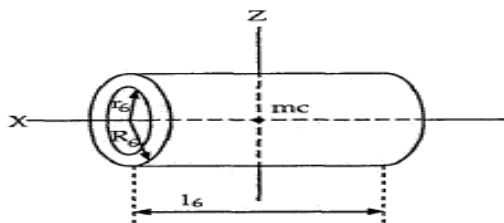


**Regular battery pack**

$$J_5 = \frac{1}{12} m_5 (a_5^2 + b_5^2)$$

$a_5$  = thickness battery pack

$b_5$  = length battery pack



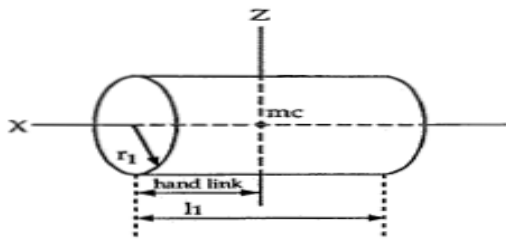
**Circular battery pack**

$$J_6 = \frac{1}{12} m_6 (3R_6^2 + 3r_6^2 + l_6^2)$$

$l_6$  = height battery pack

$r_6$  = inside radius battery pack

$R_6$  = outside radius battery pack

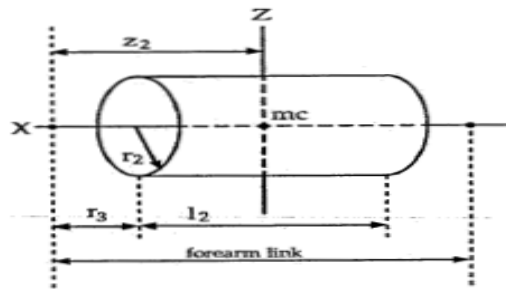


Hand

$$J_1 = \frac{1}{12} m_1 (3r_1^2 + l_1^2)$$

$$l_1 = 2 * \text{hand link}$$

$r_1$  = radius hand



Forearm

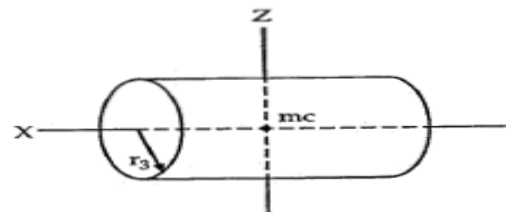
$$J_2 = \frac{1}{2} m_2 (6r_2^2 + l_2^2)$$

$$l_2 = 2 * (z_2 - r_3)$$

$$z_2 = 0.5 * \text{forearm link}$$

$r_2 = r_1$  = radius hand

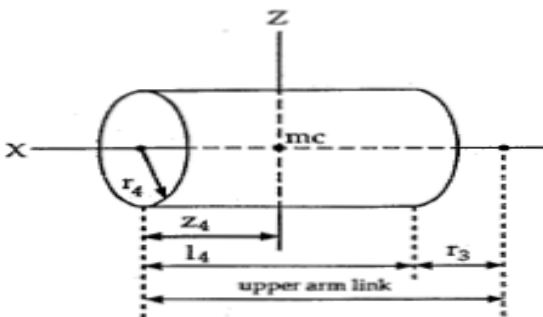
$r_3$  = radius elbow motor



Motor

$$J_3 = \frac{1}{2} m_3 r_3^2$$

$r_3$  = radius elbow motor



Upper arm

$$J_4 = \frac{1}{2} m_4 (6r_4^2 + l_4^2)$$

$$l_4 = \text{upper arm link} - r_3$$

$r_4$  = radius upper arm

Figure 3.10 Moment of inertia of common geometric shapes

## **CHAPTER 4**

### **MODEL OF HUMAN ARM**

**Approach 2: Biodynamically Modeling the upper or Lower  
Extremity**

## 4. Model of Human Arm

### 4.1 Mechanics of Human Arm

Consider the motion of an arm-forearm system illustrated in Figure 4.1.

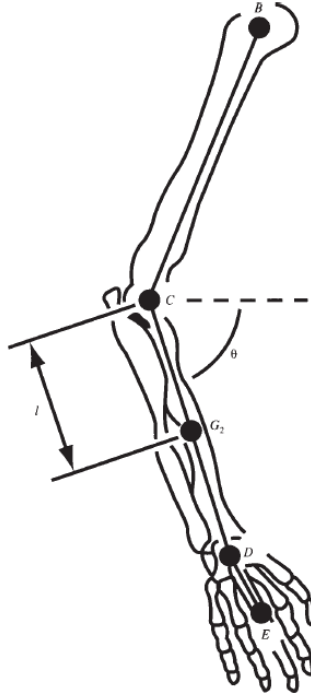


Figure 4.1 The bones of the arm, forearm, and hand with line segments superimposed

Equation of motion for the elbow joint

$$I\ddot{\theta} + mgl\cos\theta + M_{\text{applied}} = M_{\text{Elbow}} \quad (4.1)$$

Where

$I$  = mass moment of inertia of the forearm

$m$  = mass of the forearm

$M_{\text{Elbow}}$  = moment at the elbow created by muscle

$M_{\text{Applied}}$  = moment due to externally applied load

$l$  = distance from the elbow to the center of mass ( $G_2$ ) of the forearm



$\theta = \text{angle between the forearm and the horizontal plane}$

By solving for the moment created by the muscles at the elbow, an estimation of the effort required during a forearm movement activity can be determined. In order to yield estimates for each term within the equations of motion for a biodynamic system, an experimental approach involving the simultaneous collection of information from several modalities would be required. More specifically, sensors such as accelerometers (to measure acceleration or vibration), inclinometers (to measure displacement or position), load cells or force sensitive resistors (to measure applied load or grip forces), and electrogoniometers (to measure anatomic angles) should be considered. The selection of modalities, and their respective sensors, will depend upon the nature of the terms given in the equations of motion. In addition, estimates of anthropometric quantities involving mass, segment length, location of the center of mass, and the mass moment of inertia of each body segment are also required. It should be understood that these modalities might be costly to purchase and operate, and can generate large volumes of data that must be analyzed and modeled properly in order to yield practical estimates for each desired term. The results for each term can then be substituted into the equation of motion to model the dynamic behavior of the system. This approach to modeling the biodynamic of the human musculoskeletal system has proved to be extremely valuable for investigating human motion characteristics in settings of normal biomechanical function and in settings of disease.

A straightforward approach to developing dynamic analytical models of multirigid body systems that are analogous to actual anatomic systems. These models can yield overall body motion and joint forces from estimated joint angles and applied loads, and even begin to structure dynamic correlations such as those between body segment orientations and body segment kinematics and kinetics. The applications of these equations to clinical or experimental scenarios will vary tremendously.

## **4.2 The significance of dynamics**

The theory and applications of engineering mechanics is not strictly limited to nonliving systems. The principles of statics and dynamics, the two fundamental components within the study of engineering mechanics, can be applied to any biological system. They have proved to be equally effective in yielding a relatively accurate model of the mechanical state of both intrinsic and extrinsic biological structures.

In fact, nearly all of the dynamic phenomena observed within living and nonliving systems can be modeled by using the principles of rigid body kinematics and dynamics. Most machines and mechanisms involve multi-body systems where coupled dynamics exist between two or more rigid bodies. Mechanized manipulating devices, such as a robotic armature, are mechanically analogous to the human musculoskeletal system, which is an obvious multibody system. Consequently, the equations of motion governing the movement of the armature will closely resemble the equations derived for the movement of an extremity.

Careful steps must be taken in structuring the theoretical approach, particularly in identifying the initial assumptions required to solve the equations of motion. By varying any of the initial assumptions (and the justification for making them), the accuracy of the model is directly affected.

For example, modeling a human shoulder joint as a mechanical ball and socket neglects the shoulder's ability to translate and thus prohibits any terms describing lateral motion exhibited by the joint. Therefore, any such assumption or constraint should be clearly defined on the basis of the desired approach or theoretical starting point for describing the dynamics of the system. Elasticity is another example of such a constraint, and is present to some degree within nearly all of the dynamics of a biological system. Ideally, elasticity should not be avoided and will have direct implications on determining the resulting dynamic state of the system.

### **4.3 The Biodynamic significance of the equation of motion**

The equations of motion are dynamic expressions relating kinematics with forces and moments. In a musculoskeletal biodynamic system, the forces and moments will consist of joint reactions; internal forces, such as muscle, tendon, or ligament forces; or externally applied loads. Consequently, the equations of motion can provide a critical understanding of the forces experienced by a joint and effectively model normal joint function and joint injury mechanics. They can yield estimates for forces that cannot be determined by direct measurement. For example, muscle forces, which are typically derived from other quantities such as external loads, center of mass locations, and empirical data including anatomical positioning or electromyography, can be estimated.

In terms of experimental design, the equations of motion can provide an initial, theoretical understanding of an actual biodynamic system and can aid in the selection of the

dynamic properties of the actual system to be measured. More specifically, the theoretical model is an initial basis that an experimental model can build upon to determine and define a final predictive model. This may involve comparative and iterative processes used between the theoretical and actual models, with careful consideration given to every assumption and defined constraint.

Biodynamic models of the human musculoskeletal system have direct implications on device design and use and the modeling of normal and abnormal (or undesired) movements or movement patterns (the techniques with which a device or tool is used). Applications of the models can provide a better understanding for soft and hard tissue injuries, such as repetitive strain injuries (RSI), and can be used to identify and predict the extent of a musculoskeletal injury.

#### **4.4 The Lagrangian (An Energy Method) Approach**

The equations of motion for a dynamic system can be determined by any of the following four methods:

- Newton-Euler method
- Application of Lagrange's equation
- D'Alembert's method of virtual work
- Principle of virtual power using Jourdain's principle or Kane's equation

The Newton-Euler (Newtonian) approach involves the derivation of the equations of motion for a dynamic system using the Newton-Euler equations, which depend upon vector quantities and accelerations. This dependence, along with complex geometries, may promote derivations for the equations of motion that are timely and mathematically complex. Furthermore, the presence of several degrees of freedom within the dynamic system will only add to the complexity of the derivations and final solutions.

The energy method approach uses Lagrange's equation (and/or Hamilton's principle, if appropriate) and differs from the Newtonian approach by the dependence upon scalar quantities and velocities. This approach is particularly useful if the dynamic system has several degrees of freedom and the forces experienced by the system are derived from potential functions. In summary, the energy method approach often simplifies the derivation of the equations of motion

for complex multi-body systems involving several degrees of freedom as seen in human biodynamics.

#### 4.5 Introduction to Lagrange's Equation

The application of Lagrange's equation to a model of a dynamic system can be conceptualized in six steps.

- Draw all free-body diagrams.
- Determine the number of degrees of freedom in the system and select appropriate independent generalized coordinates.
- Derive the velocity for the center of mass of each body and any applicable virtual displacements.
- Identify both conservative and non-conservative forces.
- Calculate the kinetic and potential energy and the virtual work.
- Substitute these quantities into Lagrange's equation and solve for the equations of motion.

A system determined to have 'n' degrees of freedom would correspondingly have 'n' generalized coordinates denoted as  $q_k$ , where k may have values from 1 to n. A generalized, non-conservative force corresponding to a specific generalized coordinate is represented by  $Q_k$ , where k again may range from 1 to n. The derivative of  $q_k$  with respect to time is represented as Equation 4.2 shows the general form of Lagrange's equation.

$$\frac{d}{dt} \left( \frac{\partial L_1}{\partial \dot{q}_k} \right) - \frac{\partial L_1}{\partial q_k} = Q_k \quad k=1, 2, \dots, n \quad (4.2)$$

The Lagrangian L is defined as the difference between the kinetic energy T and the potential energy V:

$$L = T - V \quad (4.3)$$

After determining the Lagrangian, differentiating as specified in (4.2) will result in a set of n scalar equations of motion due to the n degrees of freedom. Since the Lagrangian approach yields scalar equations, it is seen as an advantage over a Newtonian approach. Only the velocity vector v, not the acceleration, of each body is required and any coordinate system orientation

desired may be chosen. This is a result of the kinetic energy expressed in terms of a scalar quantity as demonstrated in Eq. (4.4).

$$T = T_{Translation} + T_{Rotation} \quad (4.4)$$

$$T_{Translation} = \frac{1}{2}m(v \cdot v) = \frac{1}{2}mv^2 \quad (4.5)$$

$$T_{Rotation} = \frac{1}{2}\{w\}^T\{I_G\}\{w\} \quad (4.6)$$

For certain problems where constraint forces are considered, a Newtonian approach, or the application of both techniques, may be necessary.

#### **4.6 Biodynamically Modeling the Upper.**

In order to biodynamically model the upper extremity, we can approximate it as a rigid segment connected to a non translating cylinder.

##### **4.6.1 Two-segment model: one rigid segment connected to a nontranslating cylinder**

Consider the two-segment system shown in Figure 4.2, where a single segment of length  $l_3$  is connected to a large non-translating cylinder at point B. For initial simplicity, it is assumed that for this system, the connection of the segment is that of a revolute (or hinge) joint having only one axis of rotation. The free-moving end of the segment is identified as point C, while point  $G_1$  identifies the center of gravity for this segment. The large cylinder of height  $l_1$  and radius  $l_2$  (e.g. Torso) is fixed in space and is free to rotate about the vertical axis at some angular speed  $\Omega$ . A moving coordinate system  $b_1, b_2, b_3$  is fixed at point B and is allowed to rotate about the  $b_3$  axis so that the unit vector  $b_1$  will always lie on segment BC. This particular system considers only one segment, which can represent the upper arm or thigh, and is presented as an initial step for dynamically modeling the human upper or lower extremity. To complete the extremity model, additional segments are subsequently added to this initial segment.

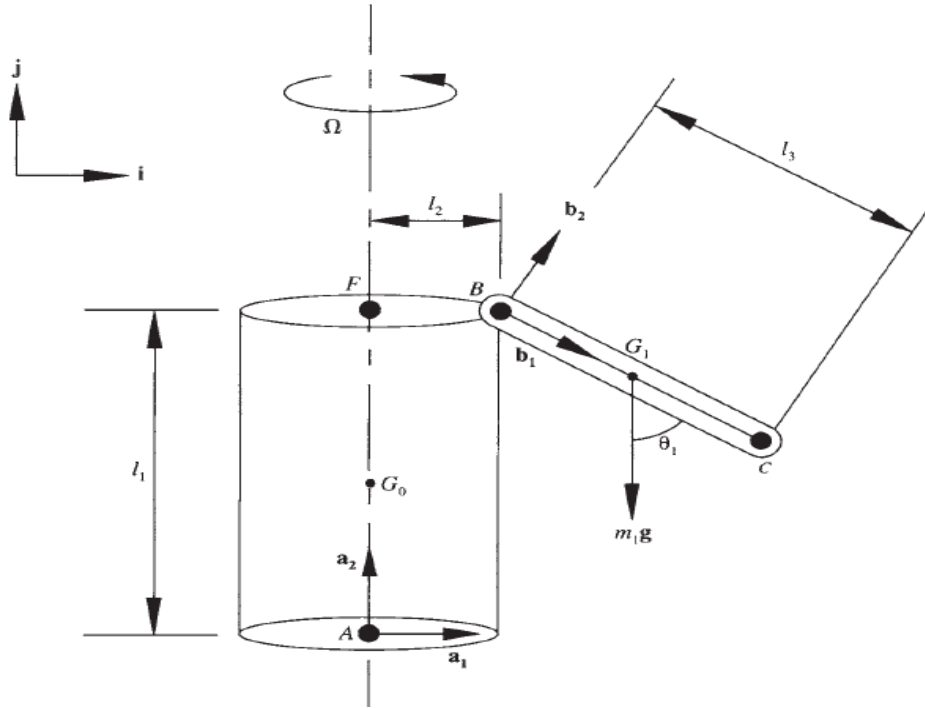


Figure 4.2 Two-segment model: one rigid segment connected to a non-translating cylinder.

The position vectors designating the locations of point B, G, and C are given as

$$r_B = l_1 + l_2 \quad (4.7)$$

$$r_{G1} = \frac{1}{2}l_3 + r_B \quad (4.8)$$

And

$$r_C = r_B + l_3 \quad (4.9)$$

respectively

The angular velocity vector of segment BC is determine to be

$$\omega_b = -\Omega \cos\theta_1 b_1 + \Omega \sin\theta_1 b_2 + \dot{\theta}_1 b_3 \quad (4.10)$$

Where

$\theta_1$  = Angle between the segment and the vertical

$\dot{\theta}_1$  = Time rate of change of that angle

The components for the mass moment of inertia about point  $G_1$  in the  $b_1, b_2, b_3$  frame of reference are

$$I_{b_1} = 0 \quad (4.11)$$

$$I_{b_2} = I_{b_3} = \frac{1}{12} m_1 l_3^2 \quad (4.12)$$

The kinetic energy of the segment BC is defined as

$$T_1 = \frac{1}{2} (I_{b_1} \omega^2_{b_1} + I_{b_2} \omega^2_{b_2} + I_{b_3} \omega^2_{b_3}) + \frac{1}{2} m_1 v_{G_1} \cdot v_{G_1} \quad (4.13)$$

Where

$v_{G_1}$  is the velocity vector of segment taken at the center of mass. This vector is determined by using the relative velocity relation

$$v_{G_1} = v_B + \omega_b \times r_{G_1/B} \quad (4.14)$$

Where  $v_B$  the velocity is vector for point B and is

$$v_B = -l_2 \Omega b_3 \quad (4.15)$$

And  $r_{G_1/B}$  is the relative position vector for point  $G_1$  as defined from point B and is

$$r_{G_1/B} = \frac{l_3}{2} b_1 \quad (4.16)$$

Substituting equation 4.16 and 4.15 into equation 4.14

$$v_{G_1} = -l_2 \Omega b_3 + (-\Omega \cos \theta_1 b_1 + \Omega \sin \theta_1 b_2 + \dot{\theta}_1 b_3) \times \frac{l_3}{2} b_1 \quad (4.17)$$

$$v_{G_1} = \frac{l_3}{2} \dot{\theta}_1 b_2 - \Omega \left( \frac{l_3 \sin \theta_1}{2} + l_2 \right) b_3 \quad (4.18)$$

So equation 4.13 can be written by using equation 4.10, 4.11, 4.12 and 4.18

$$T_1 = \frac{1}{2} \left( \frac{1}{12} m_1 l_3^2 \Omega^2 \sin^2 \theta_1 + \frac{1}{12} m_1 l_3^2 \dot{\theta}_1^2 \right) + \frac{1}{2} m_1 \left\{ \left( \frac{l_3}{2} \dot{\theta}_1 \right)^2 + \left[ -\Omega \left( \frac{l_3 \sin \theta_1}{2} + l_2 \right) \right]^2 \right\} \quad (4.19)$$

After simplification

$$T_1 = \frac{1}{24} m_1 l_3^2 \left( \Omega^2 \sin^2 \theta_1 + \dot{\theta}_1^2 \right) + \frac{1}{8} m_1 l_3^2 \dot{\theta}_1^2 + \frac{1}{2} m_1 \Omega^2 \left( \frac{l_3 \sin \theta_1}{2} + l_2 \right)^2 \quad (4.20)$$

The potential energy of the system is

$$V_1 = -m_1 g \frac{l_3}{2} \cos \theta_1 \quad (4.21)$$

Thus the Lagrange for segment BC,  $L_1$  is subsequently determined to be

$$L_1 = \frac{1}{24} m_1 l_3^2 \left( \Omega^2 \sin^2 \theta_1 + \dot{\theta}_1^2 \right) + \frac{1}{8} m_1 l_3^2 \dot{\theta}_1^2 + \frac{1}{2} m_1 \Omega^2 \left( \frac{l_3 \sin \theta_1}{2} + l_2 \right)^2 + m_1 g \frac{l_3}{2} \cos \theta_1 \quad (4.22)$$

$$\frac{\partial L_1}{\partial \theta_1} = \frac{1}{12} m_1 l_3^2 \Omega^2 \sin \theta_1 \cos \theta_1 + \frac{1}{4} m_1 l_3^2 \Omega^2 \sin \theta_1 \cos \theta_1 + \frac{1}{2} m_1 l_2 l_3 \Omega^2 \cos \theta_1 - \frac{1}{2} m_1 g l_3 \sin \theta_1 \quad (4.23)$$

After simplification

$$\frac{\partial L_1}{\partial \theta_1} = \frac{1}{3} m_1 l_3^2 \Omega^2 \sin \theta_1 \cos \theta_1 + \frac{1}{2} m_1 l_2 l_3 \Omega^2 \cos \theta_1 - \frac{1}{2} m_1 g l_3 \sin \theta_1 \quad (4.24)$$

Thus the derivative of  $L_1$  with respect to  $\dot{\theta}_1$  is

$$\frac{\partial L_1}{\partial \dot{\theta}_1} = \frac{1}{12} m_1 l_3^2 \dot{\theta}_1 + \frac{1}{4} m_1 l_3^2 \dot{\theta}_1 = \frac{1}{3} m_1 l_3^2 \dot{\theta}_1 \quad (4.25)$$

So

$$\frac{d}{dt} \left( \frac{\partial L_1}{\partial \dot{\theta}_1} \right) = \frac{1}{3} m_1 l_3^2 \ddot{\theta}_1 \quad (4.26)$$

The appropriate terms can be substituted into the Lagrange's equation

$$\frac{1}{3} m_1 l_3^2 \ddot{\theta}_1 - \frac{1}{3} m_1 l_3^2 \Omega^2 \sin \theta_1 \cos \theta_1 - \frac{1}{2} m_1 l_2 l_3 \Omega^2 \cos \theta_1 + \frac{1}{2} m_1 g l_3 \sin \theta_1 = 0 \quad (4.27)$$



Since there are no externally applied torques acting on the system in the  $\theta_1$  direction. The resulting equation of motion for the one-segment system is solved as

$$\ddot{\theta}_1 - \Omega^2 \sin\theta_1 \cos\theta_1 - \frac{3l_2}{2l_3} \Omega^2 \cos\theta_1 + \frac{3g}{2l_3} \sin\theta_1 = 0 \quad (4.28)$$

### 2.6.2 Two rigid segments connected to a non-translating cylinder

Now consider an additional segment added to the two-segment system, in figure 4.2. Assume that the additional segment added adjoins to the first segment at point C by way of a revolute joint. The new segment is of length  $l_4$ , with point D defining the free-moving end of the two-segment system and point  $G_2$  identifies the center of gravity for the second segment. An additional moving body-fixed, coordinate system  $c_1, c_2, c_3$  is defined at point C and is allowed to rotate about the  $c_3$  axis so that the unit vector  $c_1$  will always lie on segment CD.

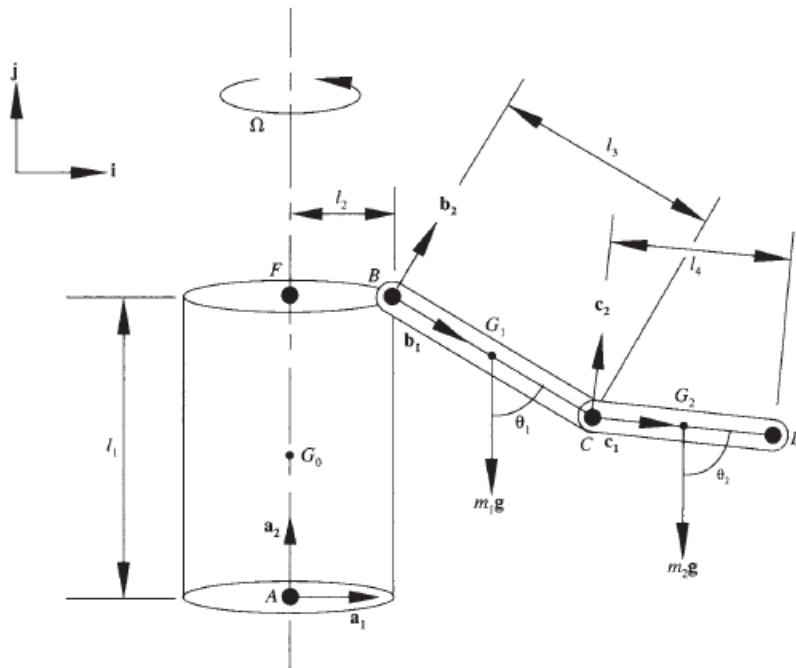


Figure 4.3 Two rigid segments connected to a non-translating cylinder

New position vectors designating the locations of point  $G_2$  and  $D$  are given as

$$r_{G_2} = \frac{1}{2}l_4 + r_c \quad (4.29)$$

$$r_D = r_c + l_4 \quad (4.30)$$

When solving a three-segment system as the one seen in Figure 4.3, the kinetic and potential energy must be determined independently for each segment. Since the kinetic and potential energy was solved previously for segment BC and is given in Equation 4.20 and 4.21, consideration needs to be given only to segment CD.

In a similar manner as before, the angular velocity vector of segment CD is determined to be

$$\omega_c = -\Omega \cos\theta_2 c_1 + \Omega \sin\theta_2 c_2 + \dot{\theta}_2 c_3 \quad (4.31)$$

Where

$\theta_2$  is the angle between the segment and the vertical and  $\dot{\theta}_2$  is the time rate of change of the angle. Also, the components for the mass moment of inertia about point  $G_2$  in the  $c_1, c_2, c_3$  frame of reference are

$$I_{c_1} = 0 \quad (4.32)$$

$$I_{c_2} = I_{c_3} = \frac{1}{12}m_2 l_4^2 \quad (4.33)$$

And the kinetic energy of segment CD is defined by the equation

$$T_2 = \frac{1}{2}(I_{c_1}\omega_{c_1}^2 + I_{c_2}\omega_{c_2}^2 + I_{c_3}\omega_{c_3}^2) + \frac{1}{2}m_2 v_{G_2} \cdot v_{G_2} \quad (4.35)$$

Where the velocity vector at point  $G_2$  is

$$v_{G_2} = v_c + \omega_c \times r_{G_2/c} \quad (4.36)$$

In order to solve Equation 4.36, the velocity vector at point C and the cross product must be determined.

$$v_C = v_B + \omega_b \times r_{C/B} \quad (4.37)$$

So that

$$v_C = -l_2 \Omega b_3 + (-\Omega \cos \theta_1 b_1 + \Omega \sin \theta_1 b_2 + \dot{\theta}_1 b_3) \times (l_3 b_1) \quad (4.38)$$

$$v_C = l_3 \dot{\theta}_1 b_2 - \Omega (l_2 + l_3 \sin \theta_1) b_3 \quad (4.39)$$

$$\omega_c \times r_{G2/C} = (-\Omega \cos \theta_2 c_1 + \Omega \sin \theta_2 c_2 + \dot{\theta}_2 c_3) \times \left(\frac{l_4}{2} c_1\right) \quad (4.40)$$

$$\omega_c \times r_{G2/C} = \frac{l_4}{2} \dot{\theta}_2 c_2 - \frac{l_4}{2} \Omega \sin \theta_2 c_3 \quad (4.41)$$

$$v_{G2} = l_3 \dot{\theta}_1 b_2 - \Omega (l_2 + l_3 \sin \theta_1) b_3 + \frac{l_4}{2} \dot{\theta}_2 c_2 - \frac{l_4}{2} \Omega \sin \theta_2 c_3 \quad (4.42)$$

Note that Equation 4.42 contains velocity terms from both moving coordinate systems  $b_1, b_2, b_3$  and  $c_1, c_2, c_3$ . Therefore, a coordinate transformation matrix is defined that will manage this

$$\begin{vmatrix} c_1 \\ c_2 \\ c_3 \end{vmatrix} = \begin{vmatrix} \cos(\theta_2 - \theta_1) & \sin(\theta_2 - \theta_1) & 0 \\ -\sin(\theta_2 - \theta_1) & \cos(\theta_2 - \theta_1) & 0 \\ 0 & 0 & 1 \end{vmatrix} \begin{vmatrix} b_1 \\ b_2 \\ b_3 \end{vmatrix} \quad (4.43)$$

From the equation 4.43 the velocity at point G2 becomes

$$v_{G2} = l_3 \dot{\theta}_1 \sin(\theta_2 - \theta_1) c_1 + [l_3 \dot{\theta}_1 \cos(\theta_2 - \theta_1) + \frac{l_4}{2} \dot{\theta}_2] c_2 - [\Omega (l_3 \sin \theta_1 + l_2) + \frac{l_4}{2} \Omega \sin \theta_2] c_3 \quad (4.44)$$

Substituting equation 4.32, 4.33 and 4.44 into 4.35, the equation for the kinetic energy of segment CD, and solving gives

$$T_2 =$$

$$\frac{1}{2} m_2 l_3^2 \dot{\theta}_1^2 + \frac{1}{2} m_2 l_3 l_4 \dot{\theta}_1 \dot{\theta}_2 \cos(\theta_2 - \theta_1) +$$

$$\begin{aligned} & \frac{1}{6}m_2l_4^2\dot{\theta}_2^2 + \frac{1}{2}m_2l_3^2\Omega^2\sin^2\theta_1 + \frac{1}{2}m_2l_3l_4\Omega^2\sin\theta_1\sin\theta_2 + m_2l_2l_3\Omega^2\sin\theta_1 + \frac{1}{2}m_2l_2^2\Omega^2 + \\ & \frac{1}{2}m_2l_2l_4\Omega^2\sin\theta_2 + \frac{1}{6}m_2l_4^2\Omega^2\sin^2\theta_2 \end{aligned} \quad (4.45)$$

And the potential energy of segment CD is determined to be

$$V_2 = -m_2g l_3\cos\theta_1 - m_2g \frac{l_4}{2}\cos\theta_2 \quad (4.46)$$

The total kinetic and potential energy of the system can be determined by summation of

$$T = T_1 + T_2 \quad (4.47)$$

And

$$V = V_1 + V_2 \quad (4.48)$$

Thus the Lagrangian for the system is

$$L = (T_1 + T_2) - (V_1 + V_2) = T - V \quad (4.49)$$

Thus by using equation 4.20, 4.21, 4.45 and 4.46, we have

$$\begin{aligned} L = & \left(\frac{1}{24}m_1l_3^2\left(\Omega^2\sin^2\theta_1 + \dot{\theta}_1^2\right) + \frac{1}{8}m_1l_3^2\dot{\theta}_1^2 + \frac{1}{2}m_1\Omega^2\left(\frac{l_3\sin\theta_1}{2} + l_2\right)^2 + \frac{1}{2}m_2l_3^2\dot{\theta}_1^2 + \right. \\ & \left. \frac{1}{2}m_2l_3l_4\dot{\theta}_1\dot{\theta}_2\cos(\theta_2 - \theta_1) + \right. \\ & \left. \frac{1}{6}m_2l_4^2\dot{\theta}_2^2 + \frac{1}{2}m_2l_3^2\Omega^2\sin^2\theta_1 + \frac{1}{2}m_2l_3l_4\Omega^2\sin\theta_1\sin\theta_2 + m_2l_3l_4\Omega^2\sin\theta_1 + \frac{1}{2}m_2l_2^2\Omega^2 + \right. \\ & \left. \frac{1}{2}m_2l_2l_4\Omega^2\sin\theta_2 + \frac{1}{6}m_2l_4^2\Omega^2\sin^2\theta_2\right) - \left(-m_1g \frac{l_3}{2}\cos\theta_1 - m_2g l_3\cos\theta_1 - m_2g \frac{l_4}{2}\cos\theta_2\right) \end{aligned} \quad (4.50)$$

So the equation of motion for the first generalized coordinate  $\theta_1$  is

$$\begin{aligned} & \left(\frac{1}{3}m_1 + m_2\right)l_3^2\ddot{\theta}_1 + \frac{1}{2}m_2l_3l_4\cos(\theta_2 - \theta_1)\ddot{\theta}_2 - \left(\frac{1}{3}m_1 + m_2\right)l_3^2\Omega^2\sin\theta_1\cos\theta_1 - \left(\frac{1}{2}m_1 + \right. \\ & \left. m_2\right)l_2l_3\Omega^2\cos\theta_1 + \frac{1}{2}m_2l_3l_4\dot{\theta}_1\dot{\theta}_2\sin\theta_1\cos\theta_2 - \frac{1}{2}m_2l_3l_4\left(\dot{\theta}_1\dot{\theta}_2 + \Omega^2\right)\cos\theta_1\sin\theta_2 + \\ & \left(\frac{1}{2}m_1 + m_2\right)gl_3\sin\theta_1 = 0 \end{aligned} \quad (4.51)$$

For the second generalized co-ordinate  $\theta_2$ , the equation of motion is

$$\begin{aligned} & \frac{1}{3}m_2l_4^2\ddot{\theta}_2 + \frac{1}{2}m_2l_3l_4\cos(\theta_2 - \theta_1)\ddot{\theta}_1 + \frac{1}{2}m_2l_3l_4\dot{\theta}_1\dot{\theta}_2\cos\theta_1\sin\theta_2 - \frac{1}{2}m_2l_3l_4(\dot{\theta}_1\dot{\theta}_2 + \\ & \Omega^2)\sin\theta_1\cos\theta_2 - \frac{1}{3}m_2l_4^2\Omega^2\sin\theta_2\cos\theta_2 - \frac{1}{2}m_2l_2l_4\Omega^2\cos\theta_2 + \frac{1}{2}m_2gl_4\sin\theta_2 = 0 \end{aligned} \quad (4.52)$$

## **CHAPTER 5**

### **TRANSMISSION DESIGN OF ELBOW ACTUATOR**

## **5 Transmission Design of Elbow Actuator**

Many artificial arms include the Myo-Electric hand and passive elbows. Myoelectric elbows can profitably substitute the passive ones only if they can guarantee: durability, low noise, adequate torque, low power consumption, low weight, easy motion control and natural movements. Most of these objectives can be reached by good mechanical design of the system. Mechanical efficiency of the mechanism is one of the key factors and can be achieved only avoiding long chains of gears.

Transmission is the most important element of the prosthesis and performance of the system highly depends by how it works. It can be based on gear mechanism, flywheels and pulleys, Belt, ropes and chain drives, a series elastic and Bowden cable based actuator or harmonic drive. I have used harmonic drive for elbow joint actuation due to its several advantageous properties. It can give back to an actuator many of the qualities that are lost when gears, belt, ropes and chain drives are introduced. Some characteristics of harmonic drives are high speed reduction ratio, free of backlash, high Precision, small no of components and ease of assembly, Small sized and light weight, high torque capacity, high efficiency and quite, vibration free operation.

A good prosthesis design has to take into account all the problems related with the interaction between human and machines. Ideally, prosthesis must be comfortable to wear, easy to put on and remove, lightweight, durable, and cosmetically pleasing. Furthermore, prosthesis must function well mechanically and require only reasonable maintenance. Since the very first need of an amputee is the social and psychological rehabilitation, patients should have a good feeling with their prosthesis. They should be able to perform daily activities without stress and excessive mental load.

### **5.1 Design of Elbow Drive (Actuator)**

My elbow drive consists of DC motor, planetary gear set and harmonic drive. The motor is run by rechargeable batteries. The motor is connected to the planetary gear set which in turn are connected to the harmonic drive. Transmission design supplies a speed reduction between the motor and the elbow hinge that moves the forearm. The planetary gear set provides a gear reduction of 3:1, the harmonic drive a reduction of 100:1. So the actuator provides the total ratio of 300:1.

## 5.2 Block Diagram:

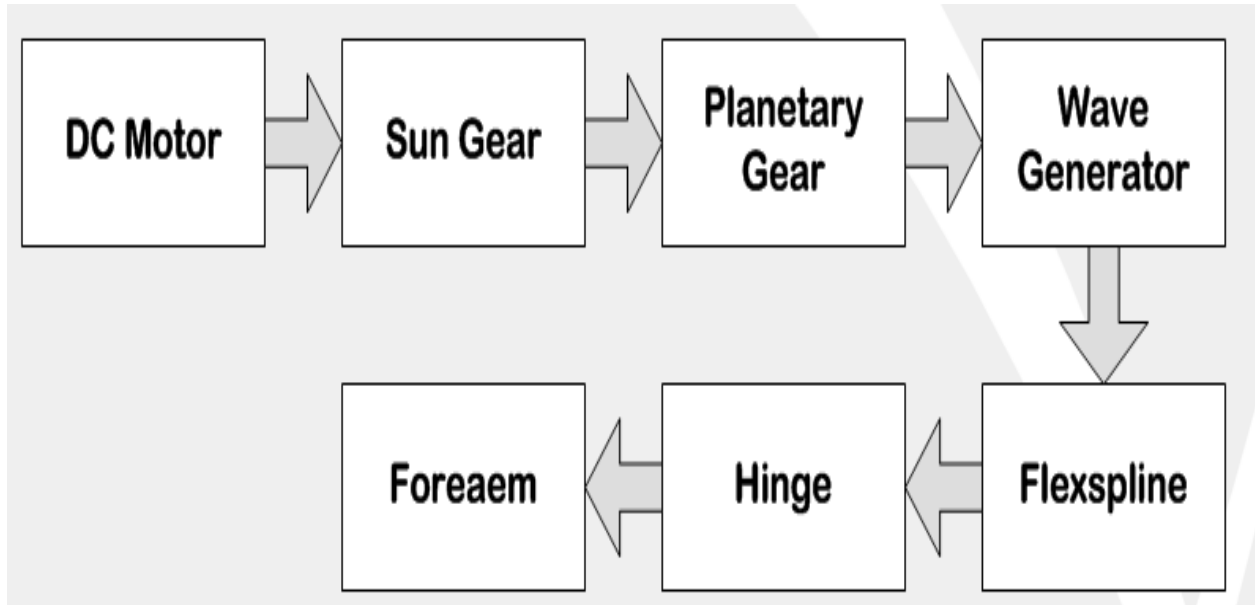


*Figure 5.1 Block diagram of elbow actuator*

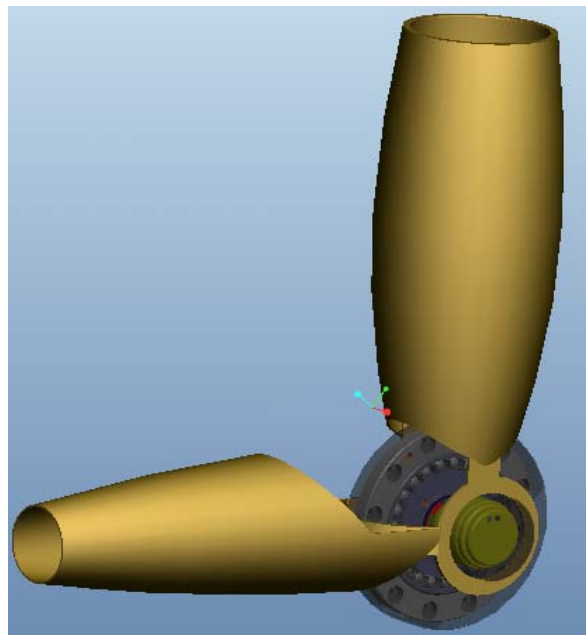


*Figure 5.2 Pro/E Model of Harmonic drive based elbow Actuator*



### 5.3 Cost Estimation

Component	Cost(USD)	Source
Harmonic Drive Model: CSD-14-100-2-AR	715	<a href="http://www.electromate.com/products/series.php?&amp;series_id=100534">http://www.electromate.com/products/series.php?&amp;series_id=100534</a> Contact Person:warren@electromate.com
Motor	4.9	RS Stock No.363-5564 Manufacturer: Astrosyn <a href="http://uk.rs-online.com/web/3635564.html#">http://uk.rs-online.com/web/3635564.html#</a>
Charger	20	BatterySpace.com/ AA Portable Power Corp. 860 South 19th street, Unit #A Richmond, CA 94804 <a href="http://www.batteryspace.com">http://www.batteryspace.com</a> <a href="mailto:sales@batteryspace.com">sales@batteryspace.com</a> Phone: 510-525-2328 Fax: 510-439-2808 <a href="http://www.batteryspace.com/compactsmartcharger04afor12v-168vnmhnicdbatterypackswithuniversal2pinmaleconnector.aspx">http://www.batteryspace.com/compactsmartcharger04afor12v-168vnmhnicdbatterypackswithuniversal2pinmaleconnector.aspx</a>
NiMH Battery Pack 12V 2200mAh	27.95	BatterySpace.com/ AA Portable Power Corp. 860 South 19th street, Unit #A Richmond, CA 94804 <a href="http://www.batteryspace.com">http://www.batteryspace.com</a> <a href="mailto:sales@batteryspace.com">sales@batteryspace.com</a> Phone: 510-525-2328 Fax: 510-439-2808
Planetary Gear Set	4	
Housing (Turntable)	5	
<b>Total</b>	<b>776.85 USD</b>	

Table 5.1 Cost Estimation

### 5.4 Components Weight of Elbow Drive

Component	Weight
Charger	122 g
Battery	311g
Motor	51g
Harmonic Drive	60g
Planetary Gear and Turntable	40g

Table 5.2 Components Weight of Elbow Drive

## **5.5 Planetary Gear Set**

Planetary gearing is a gear system consisting of one or more outer gears, or planet gears, revolving about a central, or sun gear. So planetary gear set has three main components

- The Sun gear
- The Planet gear and the planet gear carrier
- The ring gear

Each of these three components can be the input, the output or can be held stationary. Choosing which piece plays which role determines the gear ratio for the gear set.

## **5.6 Planetary Gear Set applications and advantages**

Planetary gear set can often be used in place of other styles of gear drives in a variety of applications, such as robotics painting applications, where precise motion is absolutely necessary. They have high torque, low backlash and are used in high performance applications. Some of their advantages are

- High input speed
- Low backlash
- Compact size to accommodate application where space is a limiting factor
- High Torque

## **5.7 Working Principle**

Power is transmitted from the motor to the one of the gear normally sun gear. The sun gears drive the planet gears which are uniformly spaced and rotating around the sun gear. The Planetary gears are contained within an internal tooth ring gear. Depending on the driving configuration, the number of teeth of the corresponding gears determines the reduction ratio. Due to load sharing among the planet gears, the torque carrying capacity of the planetary is high, leading to extremely high reliability and life. The transmitted power through the gear drive is not only higher in torque than what was the input, but lower in speed (the gear drive can also be used as a speed increaser/torque de-creaser).

## 5.8 Driving Configuration of Planetary Gear Set

	<b>Input</b>	<b>Output</b>	<b>Stationary</b>	<b>Calculation</b>
A	Sun (S)	Planet Carrier (C)	Ring (R)	$1 + R/S$
B	Planet Carrier (C)	Ring (R)	Sun (S)	$1 / (1 + S/R)$
C	Sun (S)	Ring (R)	Planet Carrier (C)	$-R/S$

*Table 5.3 Driving configuration of planetary gear set*

I have chosen the configuration “C”. i.e.

- Input: Sun Gear (S)
- Output: Ring (R)
- Stationary: Planet Carrier (C)

Calculations:

Ring Gear (R) = 18 teeth

Sun Gear (S) = 6 teeth

Planet Gear (P) =?

$$R = (2 \times P) + S \quad (33)$$

$$18 = (2 \times P) + 6$$

P=6 teeth

$$\text{Reduction Ratio} = -\frac{R}{S} = -3$$

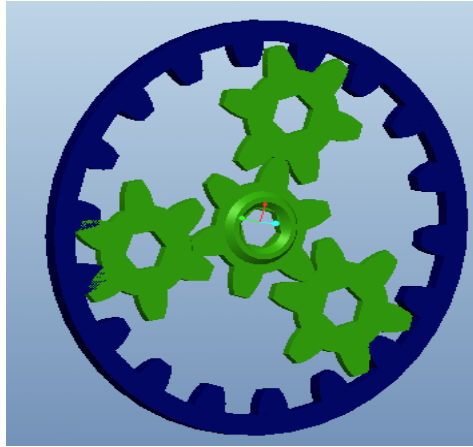


*Figure 5.3 Pro/E planetary gear set Model*

## **5.9 Harmonic Drive**

The Harmonic Drive gear has established as a “classic” robot gear, featuring zero backlash, high single-stage ratios, compact dimensions and a high torque capacity. Nearly all the world’s leading robot manufacturers apply Harmonic Drive gears in one or more of their robot versions.

### **5.10 Brief History of the Harmonic Drive Gearing**

Invented in 1959 by Walt Musser in the United States, the Harmonic Drive gear was first applied in aircraft and defense applications. The reliability, low weight and compact design were unique advantages that soon established this new gear principle in these fields. In the 1970s and 1980s the range of applications extended into industrial robotics and machine tools, where the Harmonic Drive has become de facto the standard for precise positioning drives. The 1990s saw a rapid increase in applications as requirements for increased accuracy and improved dynamic performance have necessitated the use of high quality gears and actuators, in fields as diverse as surgical robotics, measuring machines and silicon wafer processing equipment. From its origins in aerospace the Harmonic Drive gear has now established itself in robotics as the ideal solution in a wide range of different robot types. From the early 1970s, when the majority of industrial robots were still hydraulically driven, to the latest generation of highly accurate and dynamic

electrically driven robots, many of the most significant improvements in robot performance have been enabled by the continuous development of the Harmonic Drive gear.

## **5.11 Components of harmonic drive**

There are mainly three components of harmonic drive

### **5.11.1 FLEXSPLINE:**

The FLEXSPLINE is a non-rigid, steel cylindrical cup with external teeth on a slightly smaller pitch diameter than the Circular Spline. It fits over and is held in an elliptical shape by the Wave Generator. The externally toothed Flexspline is a non rigid or flexible, thin-walled, cylindrical cup which is smaller in circumference and has two less teeth than the Circular Spline. It is normally the rotating output element but can be utilized as the fixed, non rotating member when output is through the Circular Spline.

### **5.11.2 WAVE GENERATOR**

The WAVE GENERATOR is a thin raced ball bearing fitted onto an elliptical plug serving as a high efficiency torque converter. It is an elliptical cam enclosed in an antifriction ball bearing assembly. It normally functions as the rotating input element. When inserted into the bore of the Flexspline, it imparts its elliptical shape to the Flexspline, causing the external teeth of the Flexspline to engage with the internal teeth of the Circular Spline at two equally spaced areas 180 degrees apart on their respective circumferences, thus forming a positive gear mesh at these points of engagement.

### **5.11.3 CIRCULAR SPLINE**

The CIRCULAR SPLINE is a rigid ring with internal teeth, engaging the teeth of the Flexspline across the major axis of the Wave Generator. It normally functions as the fixed or non rotating member but can, in certain applications, be utilized as a rotating output element as well.

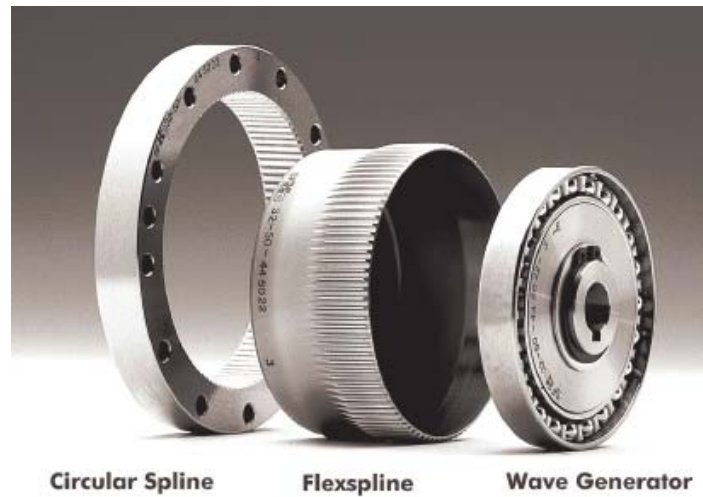


*Figure 5.4 Components of harmonic drive*

### **5.12 Principle of Operation**

As the wave generator is rotated by the primary power source, it imparts a continuously moving elliptical form or wave-like motion to the flexspline. This causes the meshing of the external teeth of the flexspline with the internal teeth of the circular spline at their two equidistant points of engagement. This meshing progresses in a continuous rolling fashion. It also allows for full tooth disengagement at the two points along the minor axis of the wave generator. Since the flexspline has two fewer teeth than the circular spline and because full tooth disengagement is made possible by the elliptical shape of the wave generator, each complete revolution of the wave generator causes a two-tooth displacement of the flexspline in relation to the circular spline. This displacement is always in the opposite direction of the rotation of the wave generator

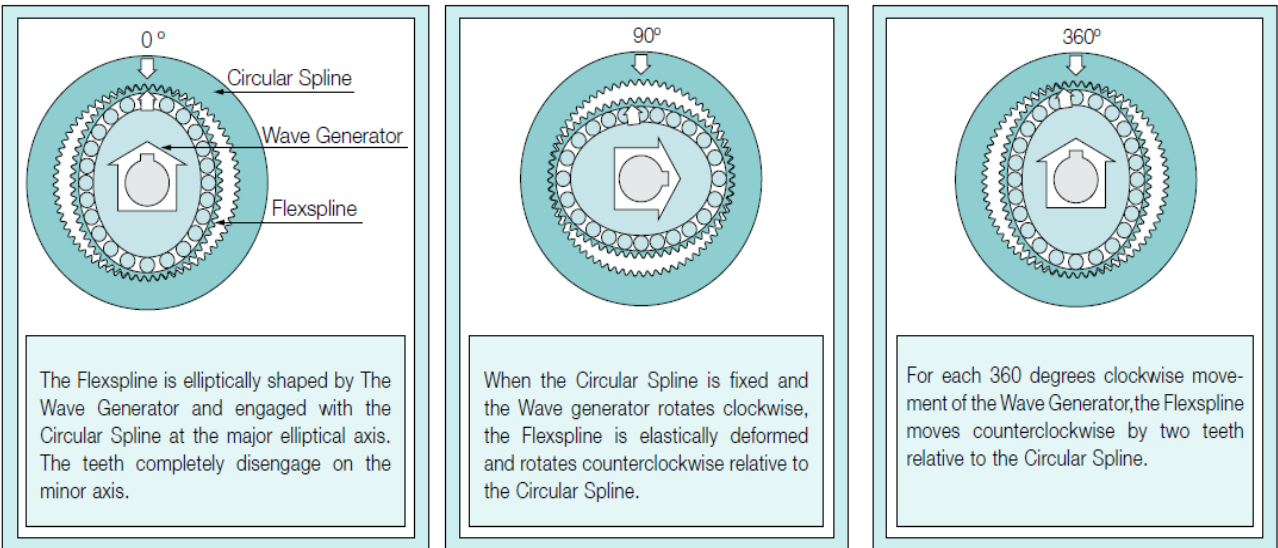


Figure 5.5 Principle of operation of harmonic drive

For example, if the wave generator is rotating in a clockwise direction, the two-tooth per revolution displacement of the flexspline will be in a counterclockwise direction, and vice-versa. In this way, a basic three-element harmonic drive component set is capable of functioning as a speed reducer. Input from a main power source through the wave generator is at a high speed, but the two-tooth per revolution displacement causes the flexspline to rotate at a considerably slower speed than the wave generator.

The reduction ratio which results can be calculated by dividing the number of teeth on the flexspline by two. For example, if a fixed circular spline has 202 teeth and an output flexspline has 200 teeth, the ratio would be  $200/(200-202) = -100:1^*$

\*The negative sign indicates that the input and output are turning in opposite directions.

### 5.13 Driving Configurations

In addition to acting as a speed reducer, a wide variety of configurations can be achieved with harmonic drive gearing by changing which element (among the wave generator, circular spline and flexspline) acts as the fixed element, input element and output element

$$R = \frac{\text{Input Speed}}{\text{Output Speed}} \quad (34)$$

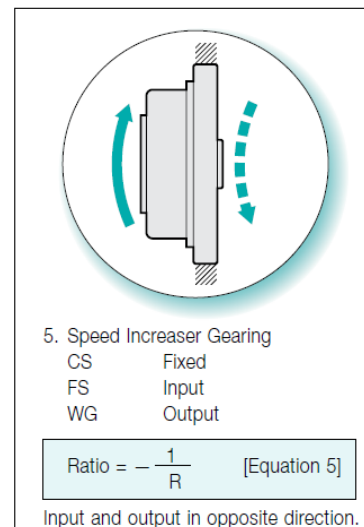
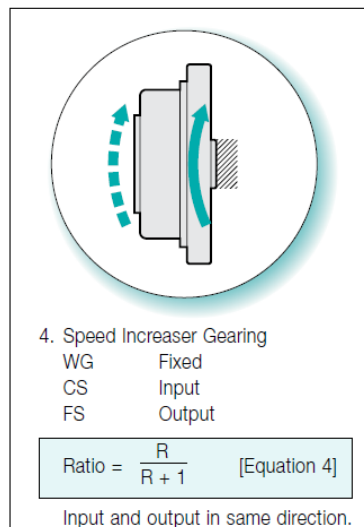
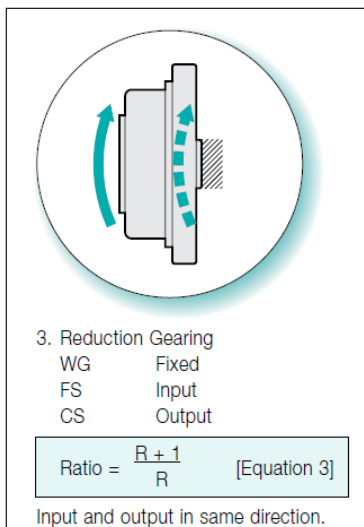
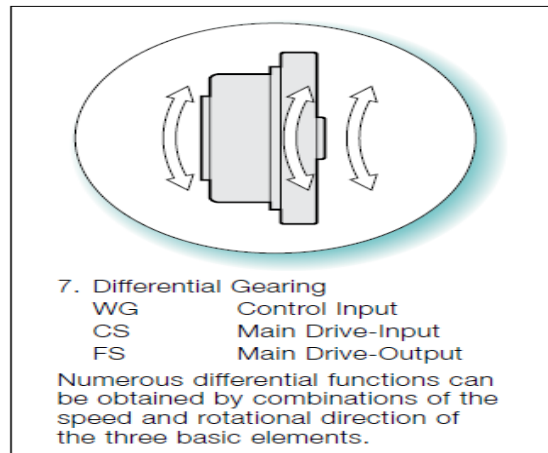
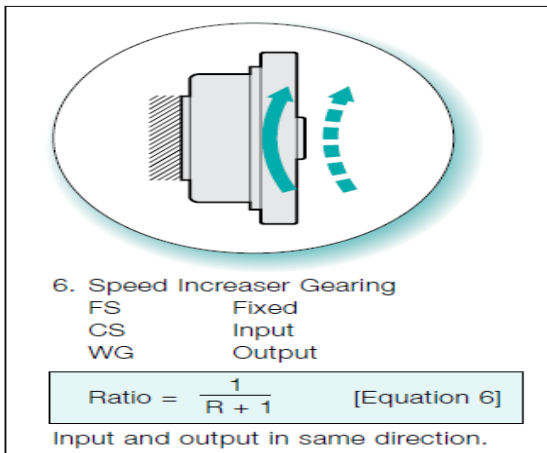
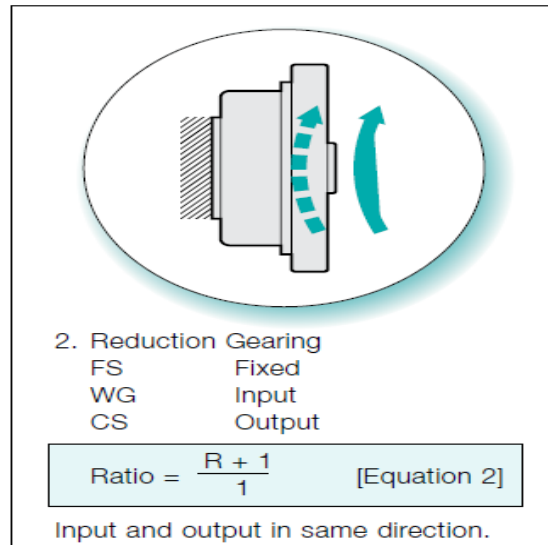
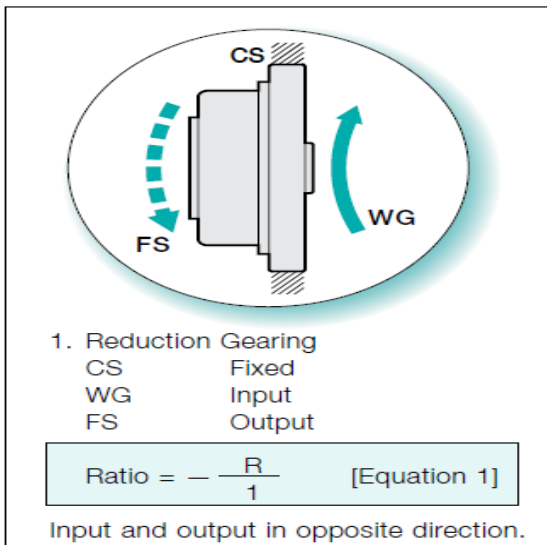


Figure 5.6 Driving Configuration of harmonic drive



## **5.14 Advantages**

The advantages of harmonic drive gearing over other, more conventional gear trains are apparent. A simple three-element construction combined with the unique harmonic drive principle puts extremely high reduction ratio capabilities into a very compact and lightweight package. This remarkable union of simplicity of construction with an operating principle that is unique also enables backlash to be held to a minimum.

### **5.14.1 Zero Backlash**

The unique design and operating principle yield some very convenient benefits. The tooth engagement motion (kinematics) of the harmonic drive gear is very different than that of planetary or spurs gearing. The teeth engage in a manner that allows up to 30% of the teeth to be engaged at all times (60 teeth engaged for a 100:1 gear ratio). This contrasts with maybe six teeth for a planetary gear set, and one or two teeth for a spur gear set. In addition, the unique kinematics allows the teeth of a harmonic drive gear to be engaged on both sides of the tooth flank. Since backlash is defined as the difference between the tooth space and tooth width, this difference is zero for harmonic drive gearing.

### **5.14.2 Consistent Performance**

As part of the design, the gear teeth of the flexspline are preloaded against those of the circular spline at the major axis of the ellipse. They are preloaded such that the stresses are well below the material's endurance limit. This has an important benefit. In conventional gearing, wear results in an increase in backlash over time. In harmonic drive gearing, as the gear teeth wear, the elastic radial deformation acts like a very stiff spring to compensate for space between the teeth that would otherwise cause an increase in backlash. This allows the performance to remain constant over the life of the gear.

### **5.14.3 High Positional Accuracy**

The combination of harmonic drive gearing principle and manufacturing technology allows positional accuracy of 30 arc-seconds ( $0.008^\circ$ ). All three gearing components (wave generator, flexspline and circular spline) are held concentric at all times. In addition, the tooth height, pitch circle and tolerances are controlled to millionths of an inch. These factors, when

combined with the 30% tooth engagement, allow for sustained accuracy far better than other gearing technologies.

#### **5.14.4 High Torque-to-Weight Ratio**

Harmonic drive gearing offers higher torque-to-weight and torque-to-volume ratios than other gearing technologies. The lightweight construction and single-stage gear ratios of up to 160:1 allow the gears to be used in applications requiring minimum weight or volume. Small motors can exploit the large mechanical advantage of a 160:1 gear ratio to create a compact, lightweight and low-cost package.

#### **5.14.5 Affordable Precision.**

Harmonic drive gearing offers many performance advantages as compared to conventional gearing technologies. Yet, it's simple and elegant design allows manufacturing costs to be roughly equal to that of other precision motion control technologies. This provides an attractive cost/benefit proposition for most motion control applications.

### **5.15 Harmonic Drive Applications:**

As indicated above, there is already a wide range of different robotic applications for Harmonic Drive gears. The new developments in the field of lightweight gear design are opening up new applications in both industrial and service robots. The following are just a few recent examples showing how lightweight Harmonic Drive gears are already being used in practice.

#### **5.15.1 SCARA Robots**

The primary axes of Scara robots are a traditional application area. Here the required speed is increasing dramatically without any compromise in accuracy. This is also necessitating the use of lightweight gears. After the development new harmonic drive gear, the lower gear mass for the elbow-joint reduces the overall mass of the arm, which allows faster cycle times. Reducing the moment of inertia of both shoulder- and elbow joint gears also allow faster acceleration and therefore reduced cycle times. During the development of a new Scara robot type lightweight gear units were tested for more than 5000 hours in a robot of the type shown in Figure 6.4. The robot exhibited consistently high accuracy during the complete endurance test

and the robot achieved faster cycle times, whilst the effective motor current was reduced by more than 10 %



*Figure 5.7 SCARA Robot*

### **5.15.2 Light Weight Robots**

Lightweight component sets are also used in the 3<sup>rd</sup> generation of lightweight robots to be developed at the Institute of Mechatronics and Robotics at the German Aerospace Center /DLR). The robot uses 7 Harmonic Drive gears in all axes and can carry a payload of 13 kg, while only weighing 13 kg itself. This relationship is currently the world's best value. Harmonic Drive gears are also used in the unique 4-fingered hand shown in Figure 7.5. Modified version of this robot is also to be used as a service robot on the International Space station.



*Figure 5.8 Light weight Robot (DLR)*

### 5.15.3 Walking Robots

Another area with expanding Harmonic Drive applications is the field of walking robots. A particularly ambitious research project is the bi-pedal robot “Johnnie”, developed by the Institute of Applied Mechanics at the Technical University of Munich. This robot features no less than 17 lightweight Harmonic Drive gears. “Johnnie” has a very high level of autonomy and can mount or avoid numerous obstacles at a walking speed of up to 2 km/hour. Johnnie is 1,8 m tall, yet weighs just 45 kg.



*Figure 5.9 Walking Robot (TU Munich)*

So Harmonic Drive gears have a long success story in demanding robotic applications. The range of applications is increasing quickly due to continuous product development, which is leading to greatly improved product performance.

## 5.16 CSD Harmonic Drive Rating Table

CSD Size	Gear Ratio R	Rated Torque at 2000 T, rpm		Limit for Repeated Peak Torque		Limit for Average Torque		Limit for Momentary Peak Torque		Maximum Input Speed		Limit for Average Input Speed		Moment of Inertia	
		Nm	in-lb	Nm		Nm		Nm		rpm		rpm		I x10 <sup>4</sup> kg·m <sup>2</sup>	J x10 <sup>5</sup> kgf·m·s <sup>2</sup>
				Nm	in-lb	Nm	in-lb	Nm	in-lb	Oil	Grease	Oil	Grease		
14	50	3.7	33	12	106	4.8	42	24	212	14000	8500	6500	3500	0.021	0.021
	100	5.4	48	19	168	7.7	68	31	274						
17	50	11	97	23	204	18	159	48	425	10000	7300	6500	3500	0.054	0.055
	100	16	142	37	327	27	239	55	487						
20	50	17	150	39	345	24	212	69	611						
	100	28	248	57	504	34	301	76* (65)	673* (575)	10000	6500	6500	3500	0.090	0.092
	160	28	248	64	566	34	301	76* (65)	673* (575)						
25	50	27	239	69	611	38	336	127 (135)	1124 (1195)	7500	5600	5600	3500	0.282	0.288
	100	47	416	110	974	75	664	152* (135)	1345* (1195)						
	160	47	416	123	1089	75	664	152* (135)	1345* (1195)						
32	50	53	469	151	1336	75	664	268 (331)	2372 (2929)	7000	4800	4600	3500	1.09	1.11
	100	96	850	233	2062	151	1336	359* (331)	3177* (2929)						
	160	96	850	261	2310	151	1336	359* (331)	3177* (2929)						
40	50	96	850	281	2487	137	1212	480 (580)	4248 (5133)	5600	4000	3600	3000	2.85	2.91
	100	185	1637	398	3522	260	2301	694* (580)	6142* (5133)						
	160	206	1823	453	4009	316	2797	694* (580)	6142* (5133)						
50	50	172	1522	500	4425	247	2186	1000 (1315)	8850 (11638)	4500	3500	3000	2500	8.61	8.78
	100	329	2912	686	6071	466	4124	1440 (1315)	12744 (11638)						
	160	370	3275	823	7284	590	5222	1577* (1315)	13956* (11638)						

Table 5.4 CSD harmonic drive rating table

**Note:** The moment of inertia:  $I=1/4GD^2$ , measured at the input

The momentary peak torque is limited by tightening torque on the flexspline.

The values in parenthesis are values in the case of the Big Bore option on the flexspline.

## **5.17 Technical Terms**

### **5.17.1 Definition of Ratings**

#### **5.17.1.1 Rated Torque ( $T_r$ )**

Rated torque indicates allowable continuous load torque at 2000 rpm input speed.

#### **5.17.1.2 Limit for Repeated Peak Torque**

During acceleration a deceleration the Harmonic Drive gear experiences a peak torque as a result of the moment of inertia of the output load. The table indicates the limit for repeated peak torque.

#### **5.17.1.3 Limit for Average Torque**

In cases where load torque and input speed vary, it is necessary to calculate an average value of load torque. The table indicates the limit for average torque. The average torque calculated must not exceed this limit.

#### **5.17.1.4 Limit for Momentary Peak Torque**

The gear may be subjected to momentary peak torques in the event of a collision or emergency stop. The magnitude and frequency of occurrence of such peak torques must be kept to a minimum and they should, under no circumstance, occur during normal operating cycle.

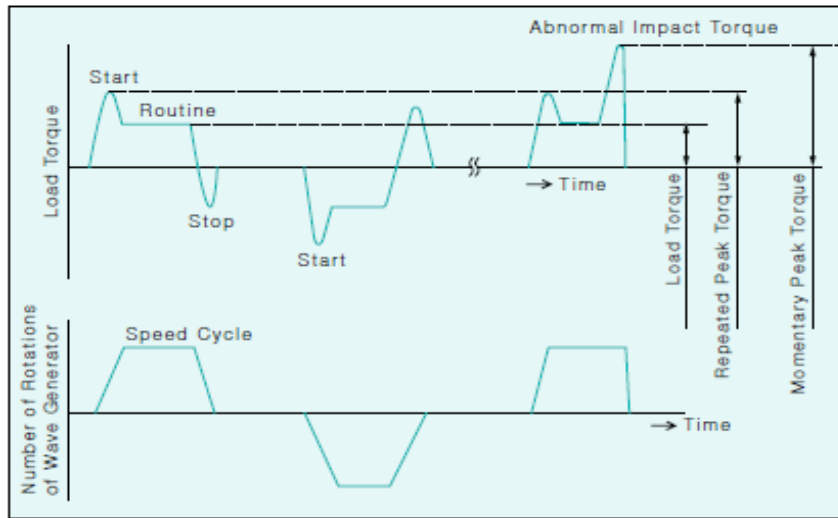


Figure 5.10 Harmonic drive rating

#### 5.17.1.5 Maximum Input Speed, Limit for average input speed

Do not exceed the allowable rating.

#### 5.17.1.6 Moment of Inertia

The rating indicates the moment of inertia reflected to the wave generator.

#### 5.17.1.7 Strength and Life

The non-rigid Flexspline is subjected to repeated deflections, and its strength determines the torque capacity of the Harmonic Drive gear. The values given for Rated Torque at Rated Speed and for the allowable Repeated Peak Torque are based on an infinite fatigue life for the Flexspline. The torque that occurs during a collision must be below the momentary peak torque (impact torque). The maximum number of occurrences is given by the equation below.

$$N = \frac{1.0 * 10^4}{2 * 60^n * t} \quad (35)$$

N: Input speed before collision

t: Time interval during collision

Please note:

If this number is exceeded, the Flexspline may experience a fatigue failure.

#### 5.17.1.8 Ratcheting phenomenon

When excessive torque is applied while the gear is in motion, the teeth between the Circular Spline and Flexspline may not engage properly. This phenomenon is called ratcheting and the torque at which this occurs is called ratcheting torque. Ratcheting may cause the Flexspline to become non-concentric with the Circular Spline. Operating in this condition may result in shortened life and a Flexspline fatigue failure.

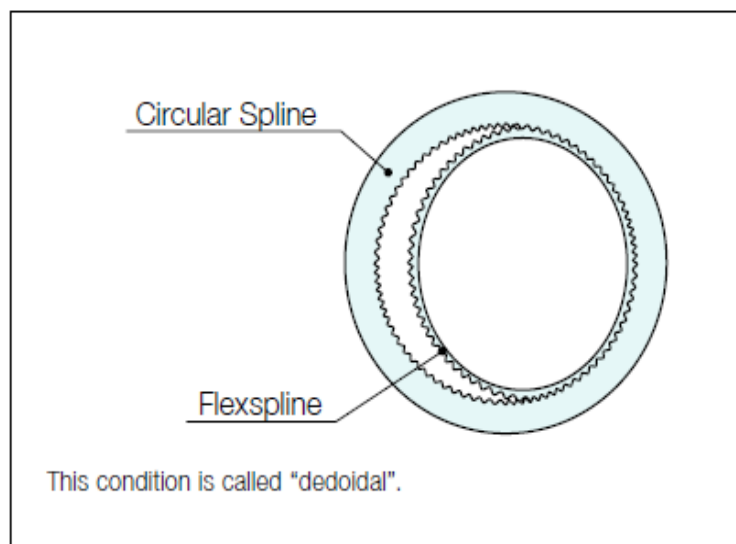


*Figure 5.11 Dedoidal condition due to ratcheting*

Note!

When ratcheting occurs, the teeth mesh abnormally as shown above. Vibration and Flexspline damage may occur. Once ratcheting occurs, the teeth wear excessively and the ratcheting torque may be lowered.

#### 5.17.1.9 CSD Ratcheting Torque (Nm)



Size	Ratio		
	50	100	160
14	88	84	-
17	150	160	-
20	220	260	220
25	450	500	450
32	980	1000	980
40	1800	2100	1800
50	3700	4100	3600

*Table 5.5 CSD Ratcheting Torque*

#### 5.17.1.10 Buckling Torque (Nm)

CSD	
Size	All Ratio
14	190
17	330
20	560
25	1000
32	2200
40	4300
50	8000

*Table 5.6 CSD Buckling Torque*

#### 5.17.1.11 The Life of a Wave Generator

The normal life of a gear is determined by the life of the wave generator bearing. The life may be calculated by using the input speed and the output load torque.

#### 5.17.1.12 Rated Lifetime $L_n$ : (n=10 or 50) hours

$L_{10}$ : CSD, SHD: 7,000

Equation for the expected life of the wave generator under normal operating conditions is given by the equation below.

$$L_h = L_n * \left( \frac{T_r}{T_{av}} \right) * \left( \frac{N_r}{N_{av}} \right) \quad (36)$$

$L_h$ : Expected Life, hours

$L_n$ : Rated Lifetime at  $L_{10}$

$T_r$ = Rated Torque

$N_r$ = Rated input speed (2000 rpm)

$T_{av}$  = Average load torque on output side

$N_{av}$  = Average input speed

### 5.17.1.13 Relative Torque Rating

The chart below shows the various torque specifications relative to rated torque. Rated Torque has been normalized to 1 for comparison.

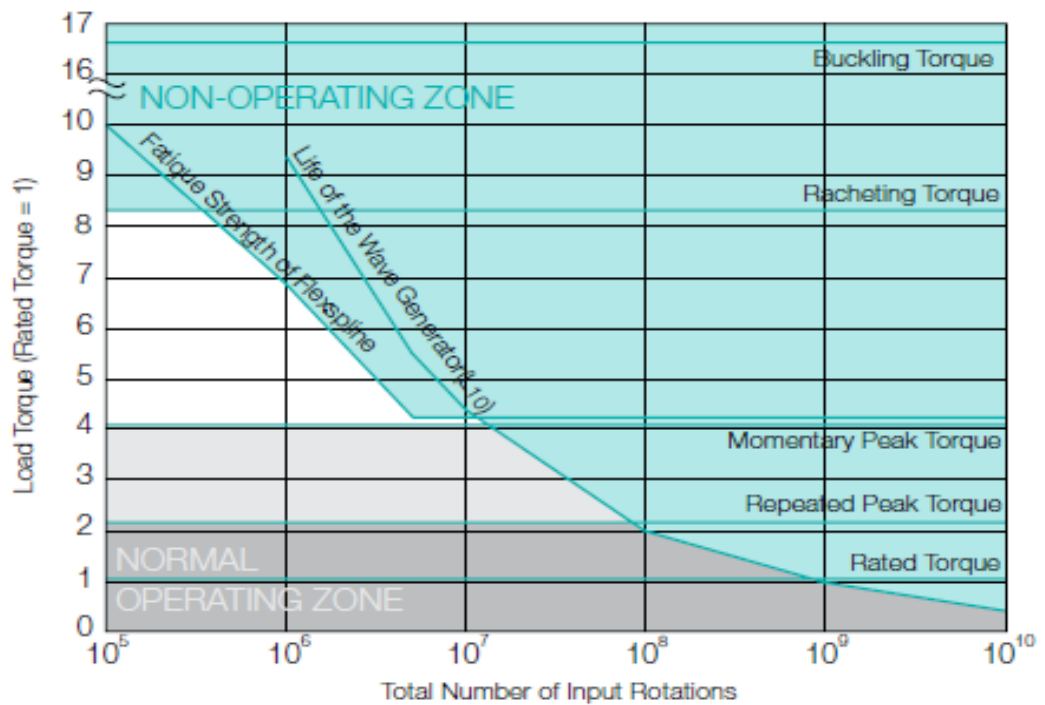


Figure 5.12 Various torque specifications relative to Load Torque

## 5.18 Selection Procedure

### 5.18.1 Size Selection

Generally, the operating conditions consist of fluctuating torques and output speeds. Also, an unexpected impact output torque must be considered. The proper size can be determined by converting fluctuating load torque into average load torque and equivalent load torque. This procedure involves selecting the size based on load torque for component sets. This procedure does not consider the life of the output bearing for housed units.

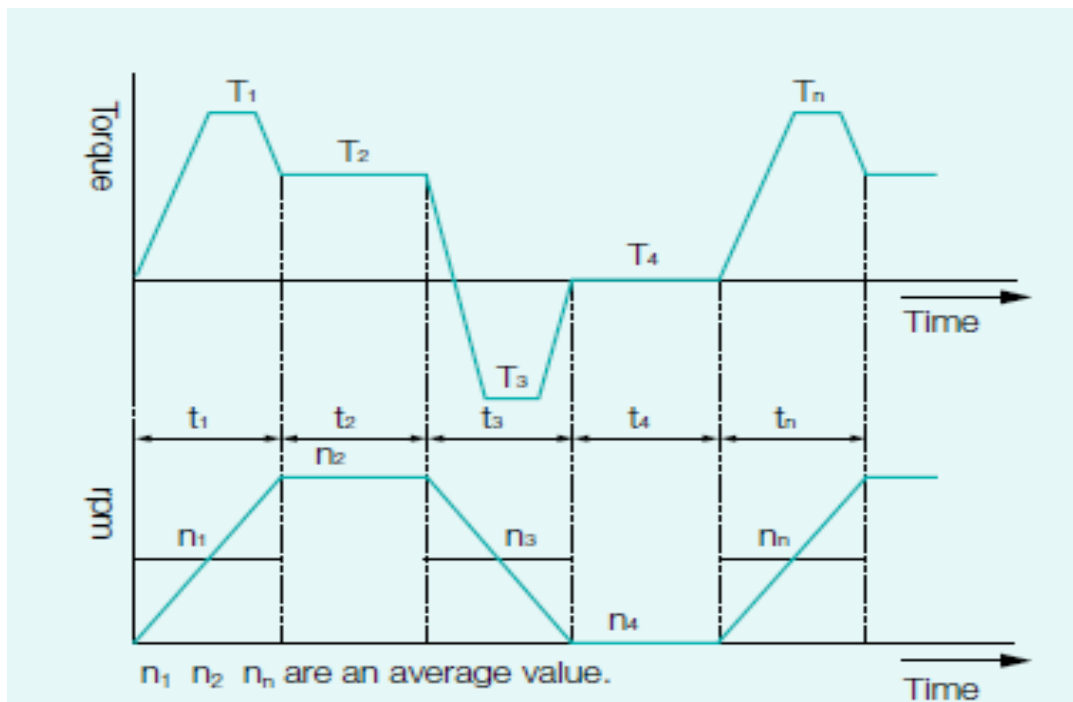


Figure 5.13 Fluctuating Torques and output speed

### 5.18.2 Parameters

Load Torque	$T_n(\text{Nm})$
Time	$t_n(\text{sec})$
Output Speed	$n_n(\text{rpm})$

### 5.18.3 Normal Operating Pattern

Acceleration	$T_1, t_1, n_1$
Regular Operation	$T_2, t_2, n_2$
Deceleration	$T_3, t_3, n_3$
Dwell	$T_4, t_4, n_4$

### 5.18.4 Maximum RPM

Max output speed	$n_0$ maximum
Max input speed	$n_i$ maximum

### 5.18.5 Impact Torque

$T_s, t_s, n_s$

### 5.18.6 Ratings

Rated Torque	$T_r$
Rated Speed	$n_r = 2000$ rpm

## 5.19 Flow Chart for selecting a size

Below flow chart is used for selecting a size. Operating conditions must not exceed the performance ratings.

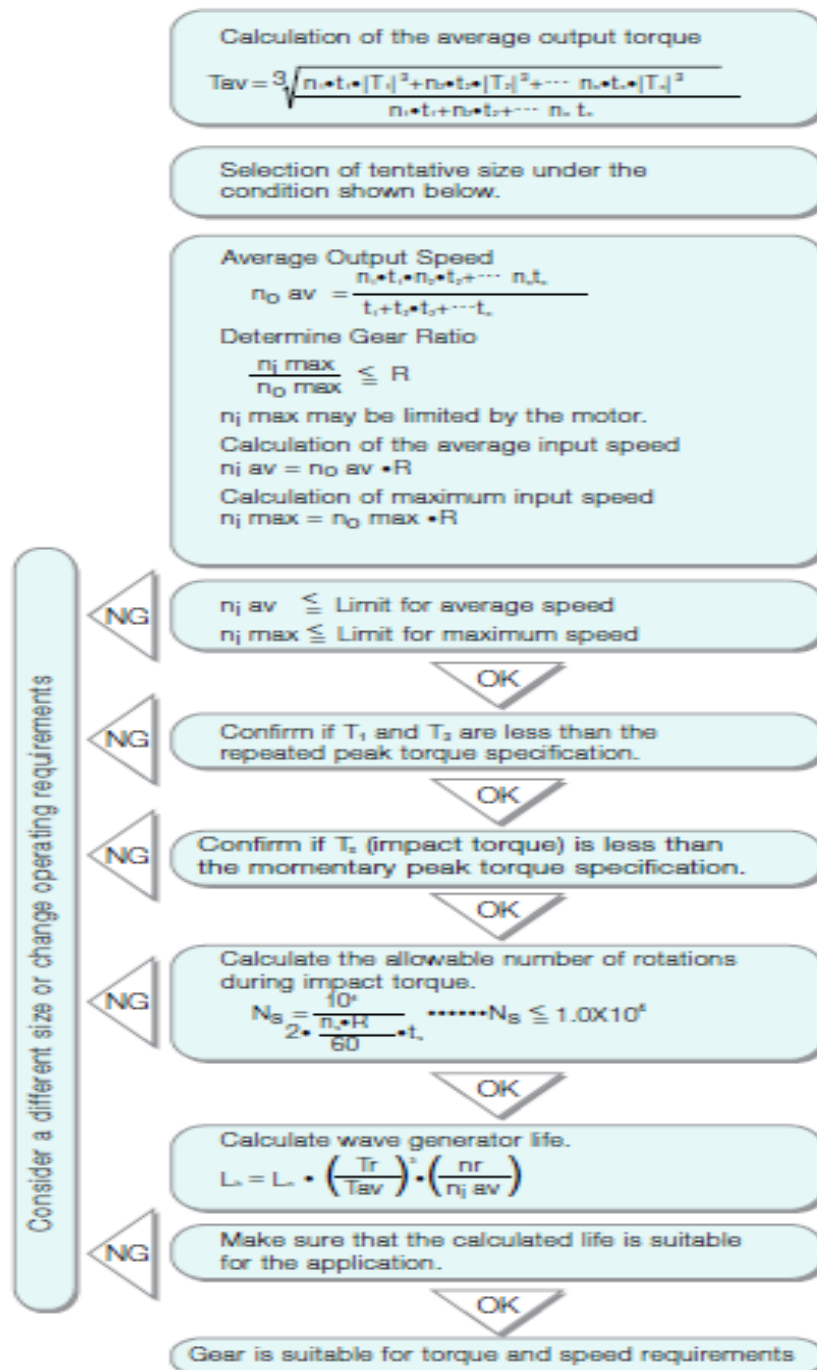


Figure 5.14 Flow chart for selecting a size of harmonic drive

## 5.20 Selection of my Harmonic Drive

I have chosen the CSD series which is compact, light weight, Zero Backlash and High accuracy and is ideal for many applications including robotics, aerospace, and factory automation. The axial length of the CSD Series has been reduced by 50% versus the CSF series. The design of the CSD component set allows the surrounding enclosure to be made very compact for additional size and weight savings.

### 5.20.1 Values of an each load torque pattern

Load Torque  $T_n = 6.9 \text{ Nm}$

Output Speed  $n_n = 18.67 \text{ rpm}$

$n_0 \text{ Max} = 18.67 \text{ rpm}$

$n_i \text{ Max} = 1867 \text{ rpm}$

Normal Operating Pattern

Acceleration  $T_1 = 6.9 \text{ Nm}$   $t_1 = 0.3 \text{ sec}$   $n_1 = 10 \text{ rpm}$

Regular Operation Stop  $T_2 = 5.49 \text{ Nm}$   $t_2 = 3 \text{ sec}$   $n_2 = 18.67 \text{ rpm}$

Deceleration  $T_3 = 3.43 \text{ Nm}$   $t_3 = 0.4 \text{ sec}$   $n_3 = 10 \text{ rpm}$

Dwell  $T_4 = 0 \text{ Nm}$   $t_4 = 0.2 \text{ sec}$   $n_4 = 0 \text{ rpm}$

$T_5 = 8.6 \text{ Nm}$   $t_5 = 0.15 \text{ sec}$   $n_5 = 18.67 \text{ rpm}$

$$T_{av} = \sqrt[3]{\frac{n_1 \times t_1 \times [T_1]^3 + n_2 \times t_2 \times [T_2]^3 + \dots \dots \dots n_n \times t_n \times [T_n]^3}{n_1 \times t_1 + n_2 \times t_2 + \dots \dots \dots n_n \times t_n}} \quad (37)$$

$$T_{av} = \sqrt[3]{\frac{10 \text{ rpm} \times 0.3 \text{ sec} \times [6.9 \text{ Nm}]^3 + 18.67 \text{ rpm} \times 3 \text{ sec} \times [5.49 \text{ Nm}]^3 + 10 \text{ rpm} \times 0.4 \text{ sec} \times [3.43 \text{ Nm}]^3}{10 \text{ rpm} \times 0.3 \text{ sec} + 18.67 \text{ rpm} \times 3 \text{ sec} + 10 \text{ rpm} \times 0.4 \text{ sec}}}$$

$$T_{av} = 5.488 \text{ Nm}$$

So

$$T_{av} = 5.488 \text{ Nm} < 7.7 \text{ Nm}$$

(For CSD-14-100-2A-GR)

$$n_{0 \text{ av}}(\text{rpm}) = \frac{n_1 \times t_1 + n_2 \times t_2 + \dots + n_n \times t_n}{t_1 + t_2 + t_3 + \dots + t_n} \quad (38)$$

$$n_{0 \text{ av}}(\text{rpm}) = \frac{10 \text{ rpm} \times 0.3 \text{ sec} + 18.67 \text{ rpm} \times 3 \text{ sec} + 10 \text{ rpm} \times 0.4 \text{ sec}}{0.3 \text{ sec} + 3 \text{ sec} + 0.4 \text{ sec} + 0.2 \text{ sec}}$$

$$n_{0 \text{ av}} = 16.15 \text{ rpm}$$

(R)

$$\frac{1867 \text{ rpm}}{18.67 \text{ rpm}} = 100 \leq R(100)$$

$$n_{i \text{ av}} = n_{0 \text{ av}} \times 100 = 16.15 \times 100 = 1615 \text{ rpm}$$

$$n_{i \text{ max}} = 18.67 \times 100 = 1867 \text{ rpm}$$

$$n_{i \text{ av}} = 1615 \text{ rpm} < 6500 \text{ rpm (For CSD-14-100-2A-GR)}$$

$$n_{i \text{ max}} = 1867 \text{ rpm} < 14000 \text{ rpm (For CSD-14-100-2A-GR)}$$

Confirm that  $T_1$  and  $T_3$  are within a

$$T_1, T_3 \text{ (Nm)}$$

$$T_1 = 6.9 \text{ Nm} < 19 \text{ Nm (For CSD-14-100-2A-GR)}$$

$$T_3 = 3.43 \text{ Nm} < 19 \text{ Nm}$$

$$T_s \text{ (Nm)} = 8.6 \text{ Nm} < 31 \text{ Nm (For CSD-14-100-2A-GR)}$$

$N_s$  Calculate an allowable number of rotations ( $N_s$ ) and confirm  $\leq 1.0 \times 10^4$

$$N_s = \frac{10^4}{2 \times \frac{18.67 \text{ rpm} \times 100}{60} \times 0.15} \quad (39)$$

$$N_s = 1071.23 < 1.0 \times 10^4$$

Calculate a life time

$$L_h = L_n * \left(\frac{T_r}{T_{av}}\right)^3 * \left(\frac{n_r}{n_{iav}}\right) \quad (40)$$

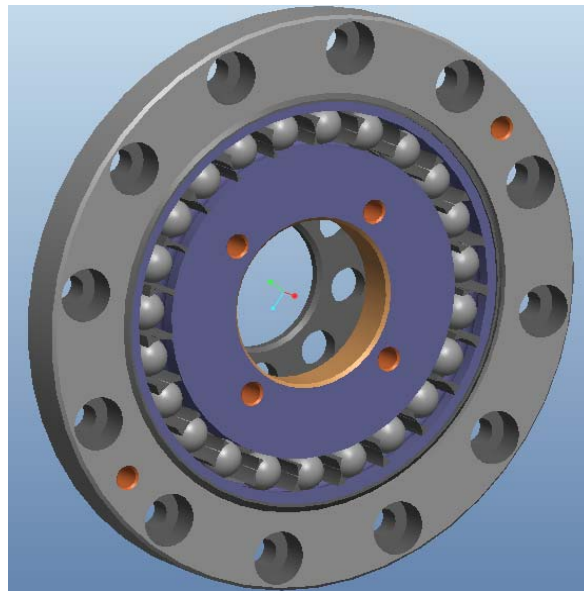
$$L_{10} = 7000 * \left(\frac{5.4}{5.488}\right)^3 * \left(\frac{2000}{1615}\right)$$

$$L_{10} = 8258 > 7000$$

So selected Harmonic Drive is

**CSD-14-100-2A-GR**

### 5.21 Pro/Engineer (Wildfire 5.0) Model





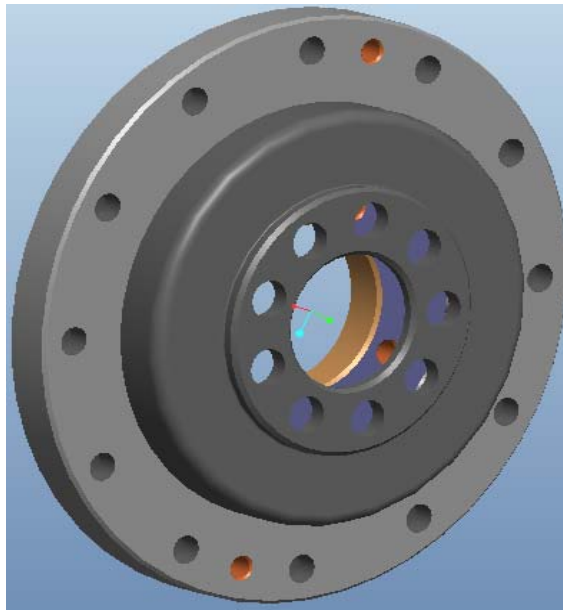


*Figure 5.15 Harmonic drive Pro/E (Wildfire 5) Model*

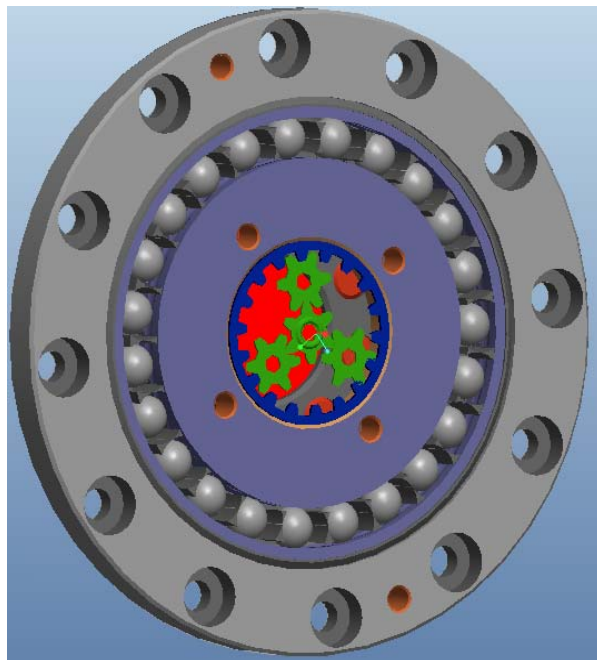


*Figure 5.16 Pro/E (Wildfire 5) Model*

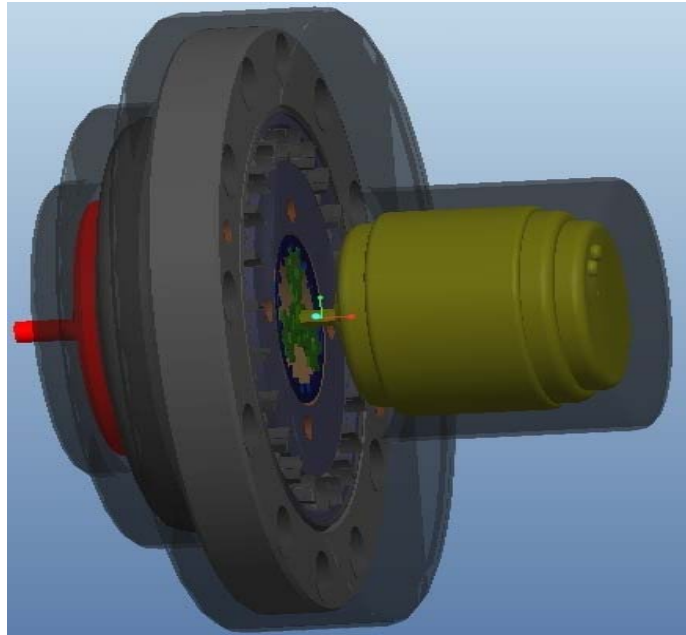


Figure 5.17 Motor, Planetary gear set, harmonic drive and housing

## 5.22 How to Order

### ORDERING CODE

Model	Size	Gear Ratio				Flexspline Configuration	*Option
CSD	20	50	100	160	2A-GR	Standard Flexspline: No Designation is Necessary	Our Application Engineers Can Assist With Any Special Configurations And Their Ordering Code
	25	50	100	160			
	32	50	100	160			
	40	50	100	160			
	50	50	100	160			
						Big Bore Flexspline: BB	
CSD	- 25	-	160	- 2A-GR	-	Blank (Standard Flexspline)	- SP*
CSD	- 25	-	160	- 2A-GR	-	BB (Big Bore Flexspline)	- SP*

Figure 5.18 Part number for ordering

## **CHAPTER 6**

### **CONCLUSIONS AND RECOMMENDATIONS**

## **6 Conclusion and Recommendations:**

The field of prosthesis is indeed a human service and covers multi dimensional learning. The Actuators usually selected for kinesthetic devices are either heavy (like direct drive electro-motors) or poor force actuators (like geared DC motors), or suffer from poor suitability for prosthesis.

The proposed actuator is high torque, light weight, compact in size, flexible and good enough to be used in real life powered prosthetic upper limb or rehabilitation exoskeletons.

The future work is the Practical implementation of designed elbow joint and results verification with “Human arm model” also the work can extends its horizon by modeling and designing actuator for shoulder joint or even for lower limb.

## References:

- [1] Federico Casolo, Simone Cinquemani and Matteo Cocetta, "Functional Design Of A Transmission For A Myoelectric Elbow Prosthesis", *Proceedings of the World Congress on Engineering 2008 Vol III WCE 2008, July 2 - 4, 2008, London, U.K.*
- [2] Thomann Sols, Solids, Structures Laboratory and V. Artigues, Tech.Innovation Evry, France, "Mechanical Design, Control Choices and first Return of Use of a Prosthetic Arm" *12th IFToMM World Congress, Besançon (France), June 18-21, 2007.*
- [3] Bram Vanderborght, Nikos G. Tsagarakis, Claudio Semini, Ronald Van Ham and Darwin G. Caldwell, "MACCEPA 2.0: Adjustable Compliant Actuator with Stiffening Characteristic for Energy Efficient Hopping" *2009 IEEE International Conference on Robotics and Automation, Kobe International Conference Center Kobe, Japan, May 12-17, 2009.*
- [4] Hoyul Lee, Chulwoo Lee, Seongjin Kim and Youngjin Choi, "New Actuator System Using Movable Pulley for Bio-mimetic system and Wearable Robot Applications", *2010 IEEE International Conference on Robotics and Automation, Anchorage Convention Distric, May 3-8, 2010, Anchorage, Alaska, USA.*
- [5] T. Gao, T. Massey, L. Selavo, M. Welsh, M. Sarrafzadeh "Participatory User Centered Design Techniques for a Large Scale Ad-Hoc Health Information System", *IEEE Computer Society, July-August 2004*
- [6] V.M.L Vossen," Evaluating the Boston Elbow, Weight distribution and motor friction experiment" *Report of a practical training at the Liberty Mutual Research Center, Hopkinton, Massachusetts, USA, and Department of Biomedical Engineering, Eindhoven University of Technology The Netherlands.*
- [7] Paul Sugarbaker, Jacob Bickers; "Above Elbow and Below Elbow Amputations", *Malware 1998.*
- [8] J. Demongeot , G. Virone, F. Duchêne, G. Benchetrit, T. Hervé, N. Noury, V. Rialle, 'Multi-sensors acquisition, data fusion, knowledge mining and alarm triggering in health smart homes for elderly people.' *Comptes rendus-Biologies, Vol. 325, Issue 6, pp 673-682, Elsevier, 2002.*
- [9] P. Blstak, M. Horvath, P. Lacko, M. Lekavy "Mobile Sleep Laboratory Body Monitoring System with EEG Sensors" *Slovak University of Technology, Bratislava, Slovakia, Jul 2007.*
- [10] Harmonic drive gear, "Cup type component sets and housed units", *Precision Gearing and Motion Control.*  
[http://www.harmonicdrive.de/cms/upload/pdf/GK2007/Katalog\\_Catalogue\\_Catalogo\\_0708.pdf](http://www.harmonicdrive.de/cms/upload/pdf/GK2007/Katalog_Catalogue_Catalogo_0708.pdf)

- [11] A.M. Weinberg, I.T. Pietsch, M.B. Helm, J. Hesselbach and H. Tscherne "A new kinematic model of pro- and supination of the human forearm" *Trauma Department of the Medical University of Hanover (MHH), Germany, Institute of Machine Tools and Production Engineering, Technical University of Braunschweig, D-38106 Braunschweig, Germany, Journal of Biomechanics 33 (2000) 487-491.*
- [12] M. Controzzi, C. Cipriani, and M. C. Carrozza, "Miniaturized non-back-drivable mechanism for robotic applications," *Mechanism and Machine Theory*, vol. 45, pp. 1395-1406, 2010, doi 10.1016/j.mechmachtheory.2010.05.008.
- [13] "Boston Digital Arm™ System."  
[http://www.liberatingtech.com/products/LTI\\_Boston\\_Arm\\_Systems.asp](http://www.liberatingtech.com/products/LTI_Boston_Arm_Systems.asp).
- [14] C. Toledo, L. Leija, R. Munoz, A. Vera, and A. Ramirez, "Upper limb prostheses for amputations above elbow: A review," in *Health Care Exchanges, 2009. PAHCE 2009. Pan American, 2009*, pp. 104-108.
- [15] S. C. Jacobsen, D. F. Knutti, R. T. Johnson, and H. H. Sears, "Development of the Utah artificial arm," *IEEE Transactions on Biomedical Engineering*, vol. 29, pp. 249-269, 1982.
- [16] E. Iversen, H. H. Sears, and S. C. Jacobsen, "Applications of control: Artificial arms evolve from robots, or vice versa," in *IEEE Control Systems Magazine*. vol. 25, 2005, pp. 16-20.
- [17] M. Fairley, "State-of-the-Art Upper-Limb Prosthetics Technology," *The O&P EDGE, 2009*.
- [18] Tustin A." The effects of backlash and of speed-dependent friction on the stability of closed-cycle control systems". *J IEE (London)*. 1947;94(II):143-51.
- [19] Heckathorne CW. Components for adult externally powered systems. In: Bowker JH, Michael JW, editors. Atlas of limb prosthetics: surgical, prosthetic and rehabilitation principles. 2nd ed., chapter 6C. St. Louis (MO): Mosby- Year Book, Inc. 1992. p. 151-74.
- [20] T. Michihiko, S. Shuji, F. Takahiro, and M. Hideo, "Fundamental Studies on the Self-locking Characteristics of Oneway Clutch," *Bulletin of JSME*, vol. 24, pp. 2154-2161, 1981-12 1981.
- [21] G. M. Roach and L. L. Howell, "Evaluation and Comparison of Alternative Compliant Overrunning Clutch Designs," *Journal of Mechanical Design*, vol. 124, pp. 485-491, 2002.